Science of the Total Environment 962 (2025) 178466

Contents lists available at ScienceDirect

Science of the Total Environment

journal homepage: www.elsevier.com/locate/scitotenv

Impact of land conversion on environmental conditions and methane emissions from a tropical peatland

Guan Xhuan Wong [a,*], Ryuichi Hirata [b], Takashi Hirano [c], Frankie Kiew [a], Joseph Wenceslaus Waili [a], Ülo Mander [d], Kaido Soosaar [d], Lulie Melling [a]

[a] Sarawak Tropical Peat Research Institute, Kota Samarahan, Malaysia
[b] Center for Global Environmental Research, National Institute for Environmental Studies, Tsukuba, Japan
[c] Research Faculty of Agriculture, Hokkaido University, Sapporo, Japan
[d] Department of Geography, University of Tartu, Estonia

HIGHLIGHTS

- Seven-year in situ measurements of environmental conditions and CH_4 flux across peat swamp forest conversion.
- Conversion substantially lowered groundwater levels, reduced soil moisture and increased soil temperatures.
- Controlled burning led to a substantial, though temporary, increase in CH_4 emissions.
- CH_4 emissions increased during conversion with drainage.
- Increased CH_4 emission was likely due to CH_4 release from drainage ditches.

GRAPHICAL ABSTRACT

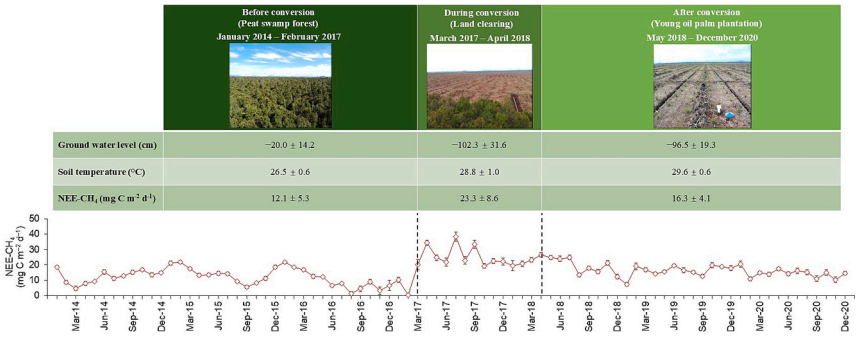

ARTICLE INFO

Editor: Yifeng Zhang

Keywords:
Peat swamp forest
Oil palm plantation
CH_4 emissions
Drainage
Histosols
Land use change

ABSTRACT

Tropical peatlands are significant sources of methane (CH_4), but their contribution to the global CH_4 budget remains poorly quantified due to the lack of long-term, continuous and high-frequency flux measurements. To address this gap, we measured net ecosystem CH_4 exchange (NEE-CH_4) using eddy covariance technique throughout the conversion of a tropical peat swamp forest to an oil palm plantation. This encompassed the periods before, during and after conversion periods from 2014 to 2020, during which substantial environmental shifts were observed. Draining the peatland substantially lowered mean monthly groundwater levels from −20.0 ± 14.2 cm before conversion to −102.3 ± 31.6 cm during conversion and increased slightly to −96.5 ± 19.3 cm after conversion. Forest removal increased mean monthly soil temperature by 2.3 to 3.1 °C, reducing net radiation (R_n) and raising vapor pressure deficit (VPD). Following the tree removal, controlled burning temporarily warmed air temperature by 8 °C, increased VPD and significantly attenuated R_n, resulting in negative values owing to radiation interception by smoke and increased surface warming. Contrary to expectations that drainage would lower CH_4 emissions, the site remained a consistent net source, with even higher emissions observed during and after conversion. The mean monthly NEE-CH_4 during conversion (23.3 ± 8.6 mg C m^{-2} d^{-1}) was about 2-times higher than before conversion (12.1 ± 5.3 mg C m^{-2} d^{-1}) and about 1.5-times higher than after

* Corresponding author.
E-mail address: wong.gx@sarawak.gov.my (G.X. Wong).

https://doi.org/10.1016/j.scitotenv.2025.178466
Received 28 August 2024; Received in revised form 30 December 2024; Accepted 8 January 2025
Available online 14 January 2025

conversion (16.3 ± 4.1 mg C m^{-2} d^{-1}). The heightened CH_4 release is likely attributable to emissions from drainage ditches, underscoring their significant role in post-conversion CH_4 dynamics. Despite its short duration, controlled burning substantially elevated NEE-CH_4, ranging from 0.04 to 0.91 mg C m^{-2} s^{-1}. Our findings highlight the substantial impact of land conversion on peatland CH_4 dynamics, emphasizing the need for accurate flux measurements across various conversion stages to refine global CH_4 budgets.

1. Introduction

Atmospheric CH_4 is the second most impactful anthropogenic greenhouse gas in terms of radiative forcing, following carbon dioxide (CO_2) and surpassing nitrous oxide (N_2O) (IPCC, 2021). Since the pre-industrial era, global mean atmospheric CH_4 concentrations have increased to >2.5 times their initial levels, rising from approximately 722 ppb in 1750 to 1890 ppb by the end of 2020 (Lan et al., 2024). Recent atmospheric CH_4 growth has been significantly influenced by both natural emissions, primarily from wetlands and anthropogenic emissions, largely attributed to agriculture, waste and fossil fuels (Jackson et al., 2020; Nisbet et al., 2023). This rise is concerning because, to adhere to the Paris Agreement's goal of keeping global warming well below 2 °C, aiming for 1.5 °C above pre-industrial levels, it is critical to curb the warming effects of CH_4 as well as to aim for net-zero or negative CO_2 emissions (Collins et al., 2018; Meinshausen et al., 2022; Cain et al., 2022). Given CH_4's short atmospheric lifespan of roughly a decade, immediate actions to decrease its emissions can quickly lower atmospheric concentrations (Ravishankara et al., 2021). Recognizing this urgency, a global effort to reduce CH_4 emissions was initiated at the Conference of the Parties 26 (COP 26) with the establishment of the Global Methane Pledge, wherein over 100 countries committed to a at least 30 % reduction in CH_4 emissions by 2030 from 2020 levels and expanded to >150 countries at COP 27 (Cael and Goodwin, 2023; Malley et al., 2023). However, intensified precipitation and rising global temperatures are predicted to increase natural CH_4 emissions from wetlands (Dean et al., 2018; Peng et al., 2022; Nisbet et al., 2023; Zhang et al., 2023). This projected surge in natural emissions could offset the efforts to reduce anthropogenic CH_4 emissions, threatening to undermine global efforts to limit warming by 2050.

Wetlands are a major source of CH_4, accounting for roughly 30 % of global emissions (Saunois et al., 2020). However, accurately estimating these emissions is challenging, creating significant uncertainty in the global CH_4 budget (Saunois et al., 2020; Basu et al., 2022; McNicol et al., 2023). This uncertainty is particularly pronounced for tropical wetlands, which are thought to be major contributors to the recent increase in atmospheric CH_4 (Dean et al., 2018; Nisbet et al., 2023; Zhang et al., 2023). In fact, a recent study suggests that tropical wetlands could be responsible for up to 72 % of all wetland CH_4 emissions (Ma et al., 2021). Improved monitoring networks, process-based modelling approaches and remote sensing techniques are crucial for reducing the uncertainty in these emissions, ultimately supporting the development of effective climate change mitigation strategies (Melton et al., 2013; Knox et al., 2019; Delwiche et al., 2021; Nisbet et al., 2022; Bansal et al., 2023). Within this context of improving emission estimates, a specific focus on tropical peatlands, particularly histosols, is crucial given their increasing extent and significant CH_4 emissions (Dargie et al., 2017; Gumbricht et al., 2017; Sakabe et al., 2018; Wong et al., 2018, 2020; Deshmukh et al., 2020).

The estimated extent of tropical peatlands has increased significantly in recent years, highlighting the dynamic nature of this ecosystem and its potential impact on the global CH_4 budget (Dargie et al., 2017; Gumbricht et al., 2017). While an earlier study estimated tropical peatland area to be 0.44 million km^2, representing 11 % of global peatland area (Page et al., 2011), recent discoveries have significantly altered this understanding. For instance, Dargie et al. (2017) identified a previously unmapped peatland complex in the Central Congo Basin, adding approximately 0.15 million km^2 to the known extent. Furthermore, Gumbricht et al. (2017) revealed extraordinary extents of peatland in the tropics, totalling 1.7 million km^2 – more than three times previous estimates of 0.44 million km^2. This trend of increasing estimates is expected to continue as new peatland areas are discovered, particularly in the tropics (Xu et al., 2018).

While tropical peatlands are a major terrestrial carbon store, our understanding of their CH_4 emissions is limited by intermittent, small-scale chamber measurements (Furukawa et al., 2005; Jauhiainen et al., 2005, 2008; Hadi et al., 2005; Melling et al., 2005). High-frequency and continuous measurements of CH_4 flux using the eddy covariance technique are essential for improving the diagnosis and prediction of terrestrial CH_4 sources to the atmosphere, as these measurements capture both short-term fluctuations and long-term trends (Delwiche et al., 2021). However, only a few studies have applied this technique in tropical peatlands, reporting net ecosystem exchange of CH_4 ranging from 0.09 to 10.8 g C m^{-2} yr^{-1} for peat swamp forests and 2.19 g C m^{-2} yr^{-1} for oil palm plantations (Sakabe et al., 2018; Wong et al., 2018, 2020; Deshmukh et al., 2020). This limited application underscores the significance of CH_4 emissions from these ecosystems and the need for more comprehensive monitoring. Although the Global Carbon Project initiated the FLUXNET-CH4 dataset to enable a global synthesis of CH_4 eddy covariance flux measurements and better constrain the global CH_4 budget, its current bias towards boreal and temperate regions, with sparse coverage in the tropics, further highlights this critical data gap (Knox et al., 2019; Delwiche et al., 2021).

Conversion of tropical peatlands for agricultural, particularly oil palm, significantly alters CH_4 emissions, with hydrological shifts both before and after conversion playing a key role in the CH_4 emission dynamics (Melling et al., 2005; Wong et al., 2020; Lam et al., 2022). These hydrological shifts influence the depth at which aerobic and anaerobic conditions occur in soils, which, in turn, control the methanogenic and methanotrophic processes that drive net CH_4 emissions (Tian et al., 2023). While these biogeochemical processes are crucial, current research on CH_4 flux primarily focuses on established ecosystems, comparing emissions between forests and mature plantations (Cooper et al., 2020). This often leads to neglecting the potentially significant emissions released during the conversion itself. For instance, controlburning of stacked woody debris during conversion represents a significant, yet overlooked source of CH_4 emissions (Hamada et al., 2013; Hirano et al., 2022). Similarly, drainage channel excavation and the resulting soil disturbance from compaction can release soil-entrapped CH_4 (Inubushi et al., 1998; Martínez-Eixarch et al., 2018). To comprehensively assess the impact of forest-to-oil palm conversion, continuous CH_4 flux measurements on an ecosystem scale are crucial. These measurements should encompass the entire conversion process, including the often overlooked but critical transient phases, capturing the full range of emission sources.

This study is of critical importance given the previously unaddressed gap in data on NEE-CH_4 during the conversion of peat swamp forests to oil palm plantations. Incorporating the NEE-CH_4 from peatland conversion into global datasets will refine CH_4 inventories for tropical peatlands and enhance the synthesis of global CH_4 flux observations (Knox et al., 2019; Delwiche et al., 2021). Our unique dataset spans seven years (January 2014 – December 2020) of continuous data, encompassing periods before, during and after conversion (peat swamp forest, land clearing and young oil palm plantation, respectively). We aim to quantify key environmental variables, including precipitation, groundwater level (GWL), soil moisture, air temperature, soil

temperature, net radiation (R_n) and vapor pressure deficit (VPD), alongside the net ecosystem exchange of CH_4 (NEE-CH_4) across these periods. This study focuses on examining their temporal variability and investigating the key hydrological drivers, specifically GWL and soil moisture, that influence NEE-CH_4 under varying conditions.

2. Material and methods

2.1. Study site

The study was carried out in Maludam Peninsula in the Betong Division of Sarawak, Malaysia (Fig. 1). The Maludam Peninsula primarily consists of tropical peatlands, covering an area of 11,744 ha, enclosed by the Batang Lupar and Batang Saribas Rivers, which flow into the South China Sea. In this region, the peat was formed ca 6000 years ago, accumulating at a rate of 0.60–1.9 mm year^{-1} (Sangok et al., 2020). The peat is particularly woody, characterized by an abundance of undecomposed woody fragments such as tree trunks, branches and roots. It reaches a depth of approximately 10 m, measured at a point 20 m from the flux tower. The regional climate is equatorial, with high temperatures, high humidity and substantial yearly precipitation. The annual rainfall pattern in Sarawak follows a distinct dry season from April to September and a wet season from October to March (Tang et al., 2020). Mean annual precipitation over 23 years (1998–2020) was 3154 ± 394 mm year^{-1} (mean ± 1 SD), measured at the Stumbin rainfall station approximately 11 km (straight-line distance) away from the study site. Mean monthly rainfall, influenced by the southwest and northeast monsoons, ranges from 167 mm in the driest month of July to 414 mm in the wettest month of December. Additionally, the mean annual air temperature recorded from 2005 to 2014 was 26.5 ± 0.2 °C (mean ± SD), measured at the nearest meteorological station located at Kuching International Airport.

Towards the end of 2010, a 40 m high flux tower was erected at the centre of the peat dome (1°23′59.42″N, 111°24′6.69″E) with the initial purpose of measuring the net ecosystem exchange of CO_2 (NEE-CO_2). Around the tower, the terrain is generally flat, with an elevation of 17 m above mean sea level. Before the conversion to oil palm plantation (January 2014 – February 2017), the 25.6 km^2 study site consisted of a

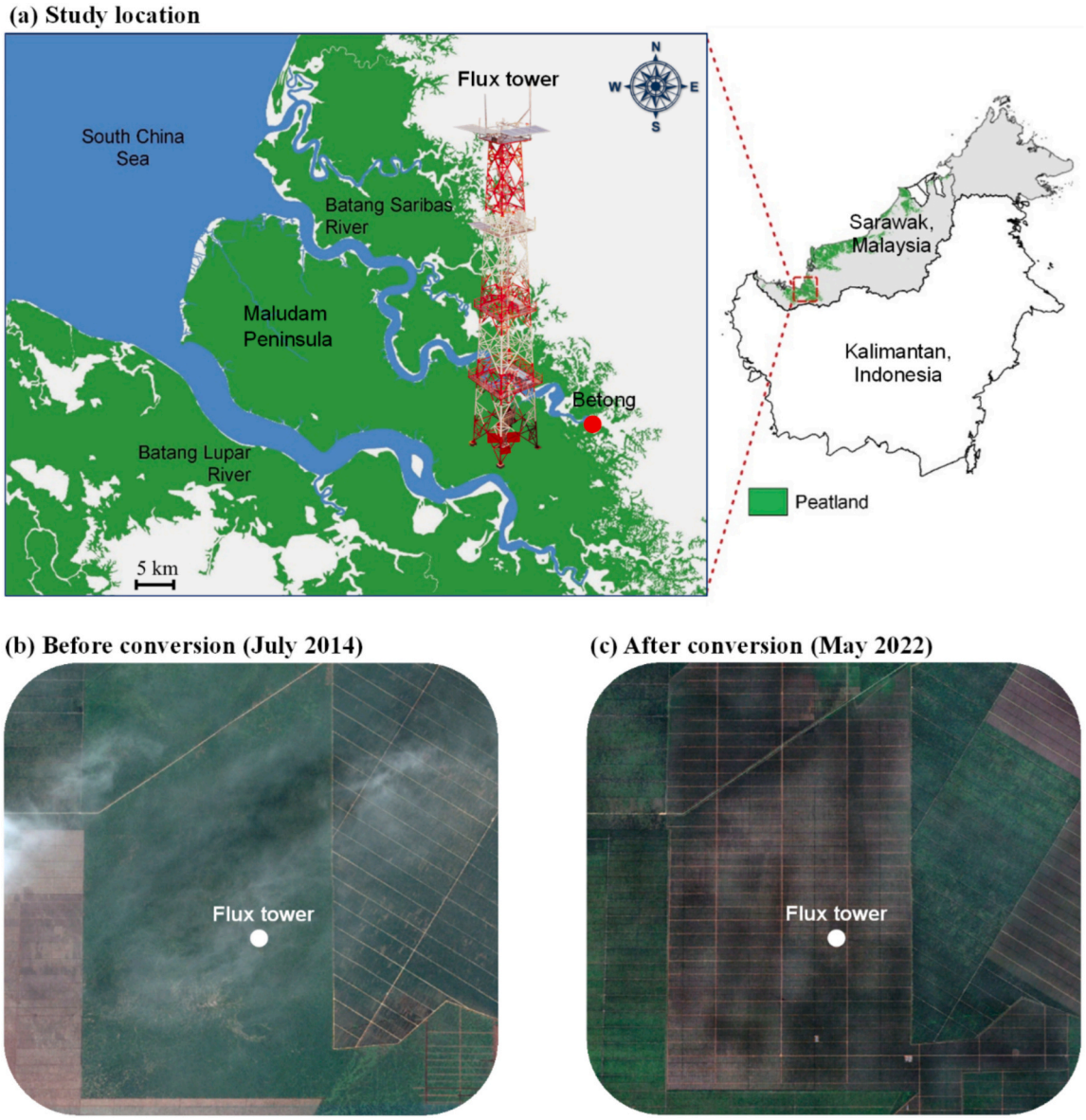

Fig. 1. (a) Map of the study location, and Google Earth satellite imagery of the area (b) before conversion depicting a secondary peat swamp forest in July 2014 and (c) after conversion showing the established oil palm plantation in May 2022.

secondary peat swamp forest (Table 1) regenerated from selective logging, located at the border of Alan Bunga and Padang Alan forests (Osaki and Tsuji, 2016; Kiew et al., 2018). The forest had a canopy height of 25 m largely due to the dominant *Litsea* spp. and *Shorea albida* trees. A dense layer of saplings formed the understory. The microtopography of the forest floor is composed of hummocks and hollows, creating an uneven surface with a thick cover of leaf litter. In 2016, the tree density was 1990 trees ha^{-1}. Since the 1990s, the area surrounding the study site has been progressively converted into oil palm plantations. The nearest plantation was 1.2 km from the study site before its conversion. Further information preceding the conversion is provided by Kiew et al. (2018).

The conversion of the secondary peat swamp forest into an oil palm plantation occurred between March 2017 and April 2018 (Table 1) through a series of land preparation steps. Initially, main drains and collection drains were constructed to lower the GWL, facilitating road construction and the clear-cutting of the forest. Trees were felled, chopped and stacked on the ground to dry before being burned in a controlled manner in February 2018. The plantation implements strict protocols for controlled burning, confining it to stacked wood in designated areas. These measures aim to prevent the fire from spreading beyond the plantation or penetrating the peat soil. During the burning, no fire spread or penetration to the soil was observed. After the controlled burning, the remaining woody debris comprising trunks, branches, twigs, stumps and coarse roots was stacked in lines along the harvesting rows. In addition, the soil was compacted to increase its bulk density, thereby preventing palm trees from leaning and toppling and improving moisture retention (Melling et al., 2008). Water gates were installed to control the GWL to support oil palm growth. In May 2018, seedlings of *Elaeis guineensis* Jacq., an African oil palm species, were planted in a triangular pattern with 8.5 m spacing between the seedlings. The compound fertilizer consisting of nitrogen, phosphorus and potassium, along with micronutrients such as copper, zinc and boron, was applied twice annually. In 2020, the height of the palm trees reached to 3 m. Overall, the study period is divided as follows: before conversion (January 2014 – February 2017), during conversion (March 2017 – April 2018), and after conversion (May 2018 – December 2020).

2.2. Measurements of fluxes and environmental variables

Measurements at the site began in December 2010 for NEE-CO_2 and in September 2012 for NEE-CH_4, both systems utilizing the eddy covariance technique. While the NEE-CO_2 throughout the conversion periods is under preparation by Kiew et al. (2025), the current study focuses exclusively on NEE-CH_4. Our CH_4 eddy covariance system consisted of an open-path CH_4 analyzer (LI-7700, Li-Cor Inc., Lincoln, NE, USA) for CH_4 concentration measurements and a 3D sonic anemometer (CSAT3, Campbell Scientific Inc., Logan, UT, USA) for measuring the three orthogonal wind components and sonic temperature. These sensors were mounted on the end of a 1 m long boom that projected towards the southeast, aligning with the predominant wind direction. Initially, the eddy covariance system was installed at the height of 41 m and repositioned to 21 m in November 2017 after the removal of forest cover. The CH_4 analyzer's lower mirror was self-cleaned daily at 4:00 am or when the relative signal strength indicator (RSSI) dropped below 20 %. However, the daily self-cleaning was insufficient to maintain data quality. Therefore, beginning in January 2014, both the lower and upper mirrors of the CH_4 analyzer were manually cleaned twice a month to increase the RSSI to 80–85 %. Data collected from September 2012 to December 2013, prior to the implementation of regular manual cleaning, were of low quality and thus excluded from this study. Raw data from the sensors were logged at 10 Hz using a datalogger (CR3000, Campbell Scientific Inc., Logan, UT, USA).

At the height of 41 m (Fig. S1, Table S1), both downward and upward shortwave and longwave radiations were measured using a net radiometer (CNR4, Kipp and Zonen, Delft, the Netherlands), while downward and upward photosynthetically active radiations were measured using quantum sensors (LI-190S, Li-Cor Inc., Lincoln, NE, USA). Wind speed and direction were measured at 41 m height using a 3-cup anemometer and wind vane (01003–5, R.M. Young Co., Traverse City, MI, USA). Air temperature and relative humidity at the heights of 3 m and initially at 41 m were measured using temperature and relative humidity probes (CS215, Campbell Scientific Inc., Logan, UT, USA) mounted in a 6-plate solar radiation shield (41303-5 A, Campbell Scientific Inc., Logan, UT, USA). The measurement setup at 41 m was later repositioned to 21 m in November 2017. Soil temperature was measured at a single point at both 5 cm and 10 cm depths using a platinum resistance thermometer (C-PTWP, Climatec, Tokyo, Japan). Soil moisture was measured in the top 10 cm and 30 cm soil layers using time domain reflectometry sensors with one replicate at each depth (CS616, Campbell Scientific Inc., Logan, UT, USA). Precipitation was measured using a tipping-bucket rain gauge (TE525, Campbell Scientific Inc.) positioned at 1 m above the ground in a nearby open space. All the environmental variables were measured every 5 s, averaged over 5-min intervals and logged with a datalogger (CR1000, Campbell Scientific Inc., Logan, UT, USA). The GWL was measured at a single point using a water level logger (HOBO, Onset, Bourne, MA, USA) installed within a perforated PVC pipe located 20 m away from the tower. All the measurement systems were powered by solar energy. In this study, only the following environmental variables are reported: precipitation, GWL, soil moisture (30 cm depth), air temperature (initially measured at the height of 41 m and later repositioned to 21 m), soil temperature (5 cm depth), R_n (41 m height) and VPD (41 m height).

Table 1
The timeline, tree density, dominant tree species, bulk density, loss on ignition and pH for the periods of before, during and after conversion. The values of bulk density, loss on ignition and pH represent mean ± SD.

Variable	Period		
	Before conversion (Peat swamp forest)	During conversion (Land clearing)	After conversion (Young oil palm plantation)
Timeline	January 2014 – February 2017	March 2017 – April 2018	May 2018 – December 2020
Tree density (trees ha^{-1})	1990	–	145
Dominant tree species	*Litsea* spp. *Shorea albida*	–	*Elaeis guineensis* Jacq
Bulk density (g cm^{-3})[a]	0.13 ± 0.01	0.14 ± 0.01	0.18 ± 0.02
Loss on ignition (%)[b]	99.2 ± 0.1	99.1 ± 0.2	98.8 ± 0.3
pH[b]	3.39 ± 0.14	3.43 ± 0.18	3.63 ± 0.13

[a] 0–5 cm soil layer.
[b] 0–25 cm soil layer.

2.3. Flux data processing and gap-filling

The eddy covariance raw data was processed to half-hourly mean CH_4 flux using Flux Calculator software (Ueyama et al., 2012). In the processing, an initial de-spiking algorithm was applied to remove data spikes in horizontal wind velocity, vertical wind velocity, CH_4 concentration and H_2O concentration (Ueyama et al., 2012). The tilt correction was applied to the sonic anemometer velocities by double rotation method (Wilczak et al., 2001). Correction for frequency loss due to line averaging and sensor separation of the open path system was performed using a theoretical transfer function (Massman, 2000, 2001). Fluctuations in CH_4 density were compensated using Webb-Pearman-Leuning correction for the effects of thermal expansion and water vapor dilution (Webb et al., 1980). The correction of the spectroscopic effect of variations in the CH_4 absorption line shape (Iwata et al., 2014; Burba et al., 2019) was performed in conjunction with the Webb-Pearman-

Leuning correction (Li-Cor Inc., 2010; McDermitt et al., 2011). In quality control, an RSSI threshold of 10 % (Alberto et al., 2014; Sakabe et al., 2018) was applied to remove low-quality half-hourly data. The CH_4 flux data were further evaluated and screened through stationary and integral turbulence tests (Foken and Wichura, 1996) and high moment test (Vickers and Mahrt, 1997; Mano et al., 2007).

The NEE-CH_4 was calculated as the sum of the CH_4 eddy flux and the storage flux, where the storage flux was calculated from CH_4 concentration measured at a single point above the canopy using the open-path CH_4 analyzer (Sakabe et al., 2018; Wong et al., 2018). Measurement of the CH_4 profile for storage flux was not feasible at our site due to the excessive power demands and associated costs. In theory, nighttime accumulation of CH_4 is expected to be balanced by its release in the morning following the onset of thermal mixing, leading to a negligible effect on daily and annual sums (Aubinet et al., 2012). The NEE-CH_4 was quality-controlled using the median absolute deviation around the median (Papale et al., 2006), ensuring the robustness of the measurements. Friction velocity (u^*) threshold was used to examine the potential underestimation of fluxes due to insufficient turbulence (Aubinet et al., 2012). Half-hourly NEE-CH_4 data were sorted into deciles based on u^* (Fig. 2) to identify a threshold where mean NEE-CH_4 at and above that u^* value showed no significant difference (indicating a plateau) (Hirano et al., 2007; Kang et al., 2019). However, Tukey's HSD test revealed no significant u^* threshold at which NEE-CH_4 values plateaued, indicating that NEE-CH_4 was independent of u^*. Therefore, a u^* threshold was not applied. Following the comprehensive quality control, 34 % of the NEE-CH_4 data were retained and qualified as high-quality data.

Data gaps in precipitation were filled with the daily rainfall data from the Stumbin rainfall station. The gaps in GWL data were filled by the tank model (Sugawara, 1979). Missing data in air temperature, soil temperature, R_n and VPD were filled using the mean diurnal variation method (Aubinet et al., 2012). The missing data in NEE-CH_4 were gap-filled using the marginal distribution sampling (MDS) method (Reichstein et al., 2005; Kiew et al., 2018; Deshmukh et al., 2020; Zhu et al., 2023). In this method, missing data were filled based on the covariation of fluxes with the environmental factors and the temporal autocorrelation within the flux data (Zhu et al., 2023). When environmental data was available, missing NEE-CH_4 was filled with the mean value of fluxes under similar environmental conditions of 2.5 cm for GWL, 0.05 m^3 m^{-3} for VWC, 1.0 °C for air temperature and 0.2 °C for soil temperature. When the environmental data was unavailable, the missing NEE-CH_4 was filled with the mean value from the same time of day, starting with ±1 h of the missing value and progressively expanding the time window (Reichstein et al., 2005). To avoid the biases due to controlled burning, the extreme values in environmental variables and NEE-CH_4 during the controlled burning were not included in data gap-filling and analysis. The data obtained during the controlled burning were presented exclusively in Sections 3.3 and 3.4 and were discussed in Sections 4.2 and 4.4. Following gap-filling, both mean eddy flux and NEE-CH_4 (eddy + storage) were calculated (Table S2). Despite the potential uncertainty associated with calculating the storage flux from a single CH_4 measurement point above the canopy, its inclusion slightly reduced mean half-hourly and annual CH_4 fluxes (mean ± 1 SD).

2.4. Global warming potential

The global warming potential (GWP, g CO_2-eq m^{-2} $year^{-1}$) was calculated for each period (before, during and after conversion) using the equation from Ishikura et al. (2018a), considering only CO_2 and CH_4 emissions:

$$GWP = \frac{FCO_2}{\alpha_{CO_2}} + \frac{FCH_4}{\alpha_{CH_4}} \times \gamma$$

where FCO_2 and FCH_4 are NEE-CO_2 (g C m^{-2} $year^{-1}$) and NEE-CH_4 (g C m^{-2} $year^{-1}$), respectively, α_{CO_2} is the ratio of molecular weight of C to CO_2, α_{CH_4} is the ratio of molecular weight of C to CH_4 and γ is the global warming potential of CH_4 over a 100 years.

The annualized NEE-CO_2 and NEE-CH_4 of the entire period before conversion, which spans 38 months, was derived by first summing all monthly values (g C m^{-2} $month^{-1}$) from January 2014 to February 2017. To calculate this, the total sum was divided by 38 to determine the average monthly value, which was then multiplied by 12 to obtain the value for an annual period. This procedure was similarly applied to the periods during and after conversion.

2.5. Statistical analysis

All statistical analyses were conducted using R statistical software (R Core Team, 2021). One-way analysis of variance (ANOVA; aov function

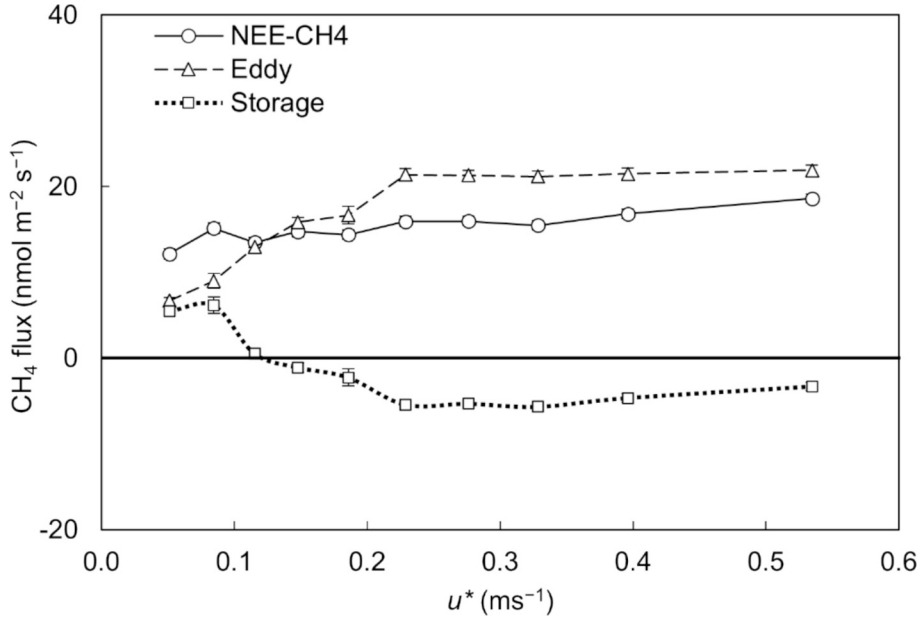

Fig. 2. Relationship of CH_4 fluxes [net ecosystem CH_4 exchange (NEE-CH_4), CH_4 eddy flux and storage flux] with friction velocity (u^*) for entire days. Half-hourly data were sorted into deciles by u^*. Vertical bars represent one standard error.

in R) was used to compare the mean values of environmental variables and NEE-CH_4 among the conversion periods, and significant differences were further examined using Tukey's HSD test. We used Pearson correlation coefficients and regression analysis to evaluate the relationships of NEE-CH_4 with GWL and soil moisture.

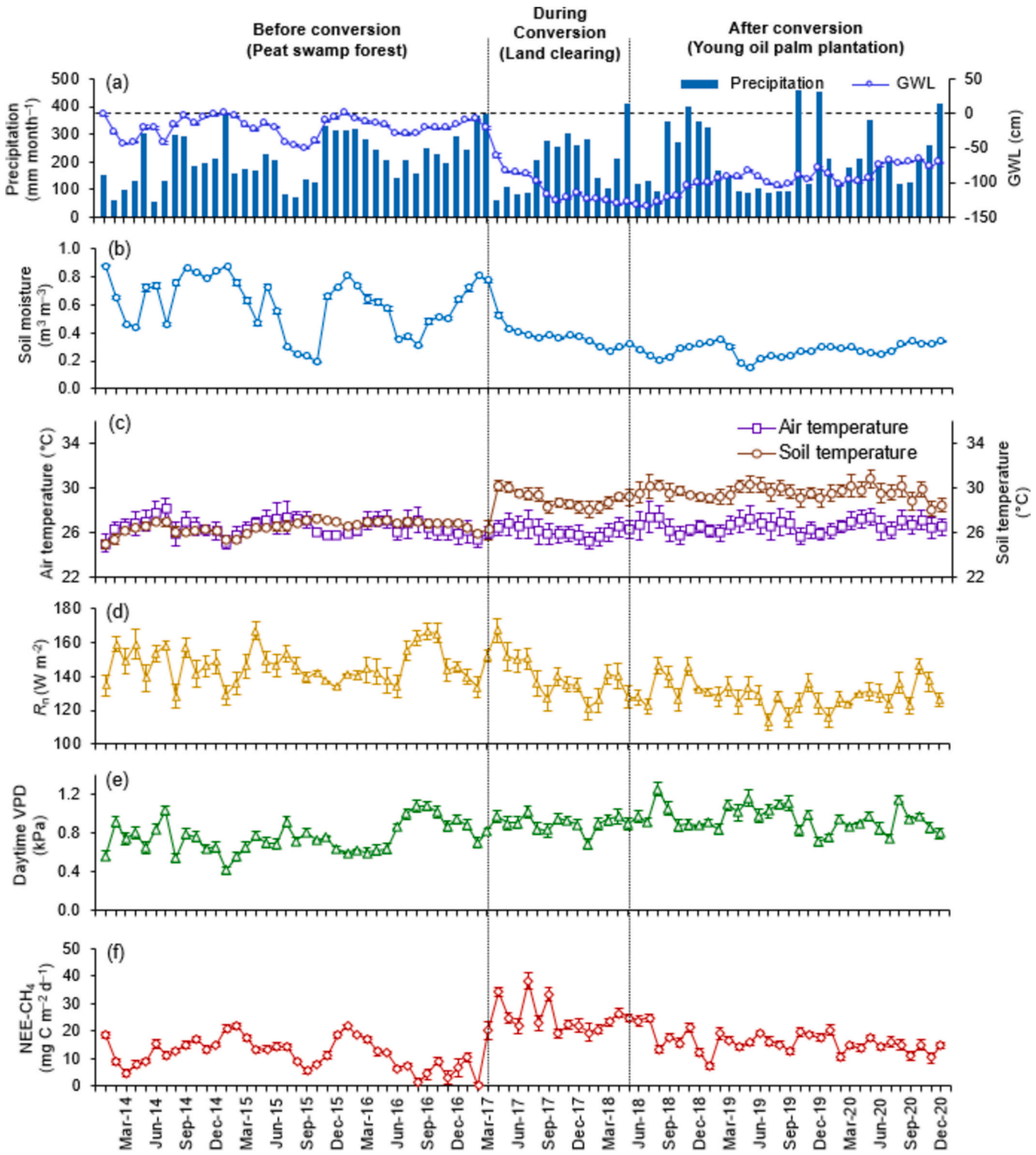

Fig. 3. Seasonal variations in monthly values of (a) precipitation and groundwater level (GWL), (b) soil moisture (30 cm depth), (c) air temperature and soil temperature (5 cm depth), (d) net radiation (R_n), (e) daytime vapor pressure deficit (VPD; 0900–1500) and (f) net ecosystem exchange of CH_4 (NEE-CH_4) from January 2014 to December 2020. The period before conversion was peat swamp forest from January 2014 to February 2017, the period during conversion was land clearing from March 2017 to April 2018, and the period after conversion was young oil palm plantation from May 2018 to December 2020. The horizontal dashed line indicates zero line. Vertical bars represent one standard error.

3. Results

3.1. Seasonal environmental variations

From January 2014 to December 2020, the monthly precipitation varied considerably, ranging from 55 to 457 mm month^{-1} (Fig. 3a). The precipitation typically increased from October to March, representing the wet season, which accounts for about 60 % of the total annual precipitation. Conversely, the months from June to August were generally the driest, with monthly precipitation falling below 150 mm. The mean annual precipitation over the study period was 2519 mm year^{-1}.

Before conversion, a distinct seasonal variation was observed in GWL, similar to those in precipitation (Fig. 3a). The monthly GWL in this period varied from −50.6 to 0.2 cm. During conversion, draining of peatland had lowered the GWL from −21 cm to −131 cm. After conversion, the monthly GWL showed a gradual increase from −129 cm in May 2018 to −71 cm in December 2020. The monthly GWL during and after the conversion were significantly lower ($P < 0.05$) compared to those before conversion (Table 2). Mean monthly GWL before, during and after conversion were − 20.0 ± 14.2, −102.3 ± 31.6 and − 96.5 ± 19.3 cm, respectively.

Seasonal variation in soil moisture was strongly influenced by precipitation before conversion (Fig. 3b). In 2015, the El Niño induced dry period from February to October led to a decline in soil moisture from 0.88 to 0.20 m^3 m^{-3}. Precipitation was particularly scarce from July to October, with only 10–14 rainy days and a significant 20-day dry spell in September. This trend reversed drastically in November with 328 mm of precipitation over 27 days, causing a sharp 0.46 m^3 m^{-3} increase in soil moisture. During and after the conversion, the soil moisture was strongly influenced by GWL. As GWL decreased due to drainage, the soil moisture simultaneously decreased to 0.15 m^3 m^{-3} in May 2019 and reverted to 0.34 m^3 m^{-3} in December 2020. The monthly variations in soil moistures during and after the conversion were narrower than before the conversion. The monthly soil moisture after conversion was significantly lower ($P < 0.05$) than before the conversion (Table 2). Mean monthly soil moisture was 0.60 ± 0.20 m^3 m^{-3} before conversion, 0.40 ± 0.12 m^3 m^{-3} during conversion and 0.28 ± 0.05 m^3 m^{-3} after conversion.

The monthly air temperature exhibited narrow variation, ranging from 25.0 to 28.1 °C in this study (Fig. 3c). Mean annual air temperature over the years 2014–2020 was 26.5 °C. There was only a minor difference (≤ 0.5 °C) in the monthly mean air temperature during the three periods, although it was significantly different ($P < 0.05$) among the periods (Table 2). Before conversion, the variation in monthly soil temperature was minimal (Fig. 3c). In April 2017, a significant increase of about 4 °C was observed due to the removal of forest cover. Higher variability in soil temperature was observed after conversion. The mean monthly soil temperature after conversion was 29.6 ± 0.6 °C, which was significantly higher ($P < 0.05$) than the soil temperature of 26.5 ± 0.6 °C before conversion (Table 2).

The monthly R_n exhibited inconsistent variation from January 2014 to December 2020 (Fig. 3d). However, after conversion, the monthly variation in R_n was narrowed compared to before conversion, and the R_n decreased significantly ($P < 0.05$; Table 2). There was no clear seasonal change in VPD, but there was a slight increase during and after the conversion (Fig. 3e). The monthly VPD was significantly higher ($P < 0.05$) during and after the conversion (Table 2).

Table 2
Mean monthly net ecosystem exchange of CH_4 (NEE-CH_4), groundwater level (GWL), soil moisture, air temperature, soil temperature, net radiation (R_n) and daytime vapor pressure deficit (VPD; 0900–1500) for the periods of before conversion (January 2014 – February 2017), during conversion (March 2017 – April 2018) and after conversion (May 2018 – December 2020). The values represent mean ± 1 standard deviation.

Variable	Period		
	Before conversion (Peat swamp forest)	During conversion (Land clearing)	After conversion (Young oil palm plantation)
NEE-CH_4 (mg C m^{-2} d^{-1})	12.1 ± 5.3 ^{a}	23.3 ± 8.6 ^{b}	16.3 ± 4.1 ^{c}
GWL (cm)	−20.0 ± 14.2 ^{a}	−102.3 ± 31.6 ^{b}	−96.5 ± 19.3 ^{b}
Soil moisture (m^3 m^{-3})	0.60 ± 0.20 ^{a}	0.40 ± 0.12 ^{b}	0.28 ± 0.05 ^{c}
Air temperature (°C)	26.5 ± 0.7 ^{ab}	26.1 ± 0.4 ^{a}	26.6 ± 0.5 ^{b}
Soil temperature (°C)	26.5 ± 0.6 ^{a}	28.8 ± 1.0 ^{b}	29.6 ± 0.6 ^{c}
R_n (W m^{-2})	146 ± 10 ^{a}	141 ± 12 ^{a}	129 ± 8 ^{b}
Daytime VPD (kPa)	0.76 ± 0.16 ^{a}	0.89 ± 0.08 ^{ab}	0.94 ± 0.13 ^{b}

Note: Different lower-case letters indicate significant differences among the three periods (ANOVA, $P < 0.05$).

3.2. Seasonal net ecosystem CH_4 exchange

Before conversion, the monthly NEE-CH_4 showed a distinct seasonal variation (Fig. 3f), with higher NEE-CH_4 during the wet season. Within this period, the monthly NEE-CH_4 were consistently positive and varied from 0.34 to 21.8 mg C m^{-2} d^{-1}. Elevated NEE-CH_4 values, exceeding 20 mg C m^{-2} d^{-1}, coincided with periods of elevated GWL, specifically 0.11 cm above ground in January 2015 and 0.16 cm in January 2016. During the conversion period, from March to September 2017, the NEE-CH_4 fluctuated considerably, between 20.1 and 38.3 mg C m^{-2} d^{-1}, followed by a minimal variation until April 2018. There were notable peaks in NEE-CH_4 during the early conversion period, specifically in March, June and August 2017. After conversion, the NEE-CH_4 decreased from 24.9 mg C m^{-2} d^{-1} in May 2018 to 14.6 mg C m^{-2} d^{-1} in December 2020. The mean monthly NEE-CH_4 during and after conversion were significantly higher ($P < 0.05$) than before conversion despite the GWL being lowered by drainage (Table 2). Mean monthly NEE-CH_4 before, during and after conversion were 12.1 ± 5.3, 23.3 ± 8.6 and 16.3 ± 4.1 mg C m^{-2} d^{-1}, respectively. While the GWL exhibited an upward trend after conversion, the NEE-CH_4 gradually decreased over time. From 2014 to 2020, the annual NEE-CH_4 varied between 3.67 and 8.25 g C m^{-2} year^{-1} with a mean of 5.74 g C m^{-2} year^{-1} (Fig. 4).

3.3. Effect of controlled burning on environmental variables

The controlled burning was carried out on the afternoon of 17 February 2018, from 15:00 to 19:00, following six consecutive rain-free days. A radius of approximately 25 m around the tower was intentionally left unburned to safeguard the sensors. No significant changes were observed in GWL, soil moisture, or soil temperature during the controlled burning (Figs. 5a – 5b) as these sensors were located in the unburned area. Nevertheless, the burning strongly influenced the aboveground measurements such as air temperature, net radiation and VPD. The effect of controlled burning was initially noted in R_n, with a drop in R_n from 436 to 102 W m^{-2} from 15:00–15:30 (Fig. 5c). The smoke generated from the burning reduced R_n to its lowest value of −790 W m^{-2} at 16:30–17:00. As the burning approached the tower area, the air temperature began to rise from 32 to 35 °C between 16:00 and 16:30, reaching a peak of 40 °C between 16:30 and 17:00, and then slowly decreased to 29 °C between 18:30 and 19:00 (Fig. 5b). The VPD showed a similar trend with air temperature. It increased from 2.29 kPa at 16:00–16:30 to a peak of 5 kPa at 16:30–17:00, and then gradually declined to 1 kPa at 18:30–19:00 (Fig. 5d).

3.4. Effect of controlled burning on NEE-CH_4

Fire-driven processes are clearly reflected in the fluctuations of

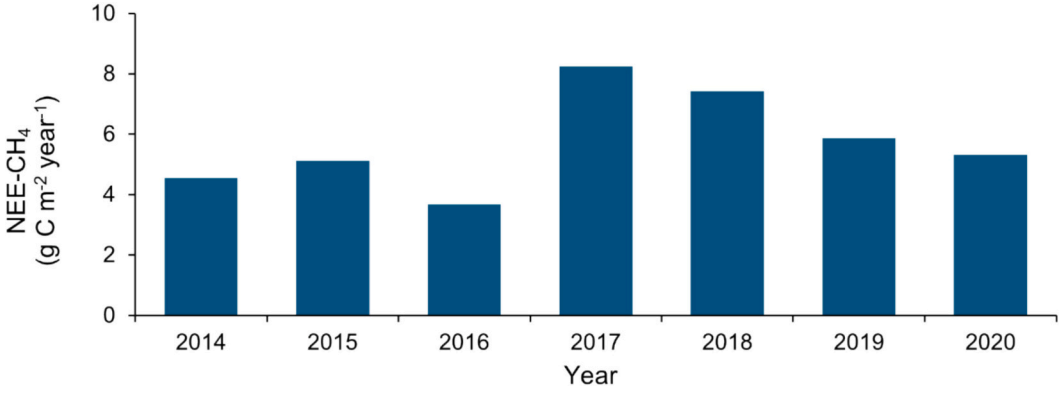

Fig. 4. Variation in annual net ecosystem exchange of CH_4 (NEE-CH_4) from 2014 to 2020.

atmospheric CH_4 concentrations. The exceptionally high NEE-CH_4 observed during the controlled burning were identified as outliers and removed by median absolute deviation (MAD) in data quality control. Thus, the NEE-CH_4 data prior to MAD filtering was used to illustrate how burning affects NEE-CH_4 (Fig. 5e). The RSSI of these data was 11–16 %, which was greater than the predefined 10 % threshold (Sakabe et al., 2018). On 17 February 2018, the NEE-CH_4 values were generally below 0.002 mg C m^{-2} s^{-1}, except for the period of controlled burning (15:00–19:00), when the values spiked significantly. During this period, the NEE-CH_4 remained relatively stable from 15:00 to 17:00, followed by a sharp increase to four extreme values of 0.91, 0.28, 0.13 and 0.04 mg C m^{-2} s^{-1}. Subsequently, after the controlled burning, these elevated values rapidly decreased to 0.00016 mg C m^{-2} s^{-1} at 19:00–19:30.

3.5. Correlation between NEE-CH_4 and hydrological variables

We examined the responses of CH_4 flux to changes in GWL and soil moisture using binned data, dividing the data into 10 groups (Figs. 6a – 6b). Before conversion, NEE-CH_4 was strongly correlated with both GWL and soil moisture ($P < 0.001$), with Pearson correlation coefficients of 0.91 and 0.98, respectively. During the conversion, the NEE-CH_4 showed a positive correlation with both GWL and soil moisture. However, only the relationship with GWL was statistically significant ($P < 0.05$), with a moderate coefficient of 0.67. After the conversion, the relationship between NEE-CH_4 and GWL became negatively associated ($P < 0.05$), while soil moisture showed no significant correlation with NEE-CH_4 ($P > 0.05$).

4. Discussion

4.1. Environmental response to land conversion

Before conversion, the variation in GWL was strongly influenced by precipitation (Fig. 3a). This pattern reflects the typical hydrology of peat swamp forests, where the GWL stays at or above the soil surface during the wet season and drops to below −30 cm during the dry season (Hirano et al., 2014; Rossita et al., 2018; Tang et al., 2020). However, following drainage during conversion, the influence of precipitation on GWL declined, indicating a shift in the hydrological pattern due to the land conversion. For instance, an increase in precipitation from 85 mm $month^{-1}$ in July 2017 to 253 mm $month^{-1}$ in October 2017 during the conversion was accompanied by a decrease in GWL, contrary to a typical GWL rise. To clearly delineate the hydrological change, we assess the distribution of daily GWL before, during and after conversion in relation to dry (April–September) and wet (October – March) seasons (Fig. 7a). During conversion, the mean GWL was remarkably lower during the wet season than in the dry season, contrasting with before conversion. The drainage during and after conversion induced greater variability in daily GWL, particularly in the dry season, as indicated by a wider interquartile range and longer whiskers. The increased variability in daily GWL could be attributed to the GWL control implemented by the plantation. Overall, the mean GWL in the young oil palm plantation after conversion (Table 2) was considerably lower than the −33 to −75 cm range reported for Southeast Asian oil palm plantations established on peatlands (Carlson et al., 2015; Junedi et al., 2017; Adhi et al., 2021).

Consistent with previous studies, our results indicated a significant reduction in soil moisture associated with the decline in GWL (Price, 1997; Zhang et al., 2022; Zhao et al., 2023). The removal of forest cover results in greater ground light exposure and increased soil temperatures, which can increase evaporation rates and further reduce soil moisture (Voldoire and Royer, 2004; McCarthy and Brown, 2006; Lin et al., 2017). Notably, the extensive daily variations in soil moisture before conversion (Fig. 7b) could be attributed to the high porosity of peat soil, characterized by its large, interconnected macropores. These macropores are known to facilitate rapid water movement within the soil layers (Baird, 1997; Holden, 2009; Wallage and Holden, 2011; Rezanezhad et al., 2016; McCarter et al., 2020), which can potentially accelerate moisture loss on dry days, resulting in high variability in soil moisture. Drainage of peatlands typically leads to soil consolidation and a consequent decrease in pore space, which narrows the range of soil moisture fluctuations both during and after conversion (Kechavarzi et al., 2010; Imran et al., 2022).

Conversion of peat swamp forests to large-scale plantations can substantially increase air and soil temperatures (Hardwick et al., 2015; Meijide et al., 2018; Anamulai et al., 2019). In this study, the air temperature measured above the canopy did not exhibit a significant increase after conversion (Table 2). However, below the canopy, at 3 m above ground, a significant rise of 1.2 °C in daily maximum air temperature was observed, as reported by Kiew et al. (2025). As for soil temperature, there was a temperature increase of 2.3 °C during conversion and 3.1 °C after conversion compared to before conversion (Table 2). This rise can be attributed to the removal of forest cover, allowing solar radiation to directly reach the soil surface, where it is absorbed and heats the soil, thereby increasing soil temperature (Potter, 1999; Laurance and Useche, 2009). In comparison with other studies, the soil temperature after conversion was 0.9–3.5 °C higher than those reported in 4–13 years of oil palm plantations on peatlands (Ishikura et al., 2018b; Swails et al., 2019; Gusmayanti et al., 2019). This discrepancy could be due to the presence of understory vegetation cover in mature plantations. Such vegetation cover reduces the amount of direct solar radiation reaching and heating the soil surface, contrasting with the conditions observed in newly established plantations.

Recent studies have highlighted the significant influence of land use changes on R_n, particularly through alterations in the upward shortwave and longwave radiations (Liu et al., 2019; Ferreira et al., 2020; Chilukoti and Xue, 2021). Consistent with these findings, our results indicate that the conversion of peat swamp forest to oil palm plantation led to a significant decrease in R_n (Table 2). The decline was due to the removal

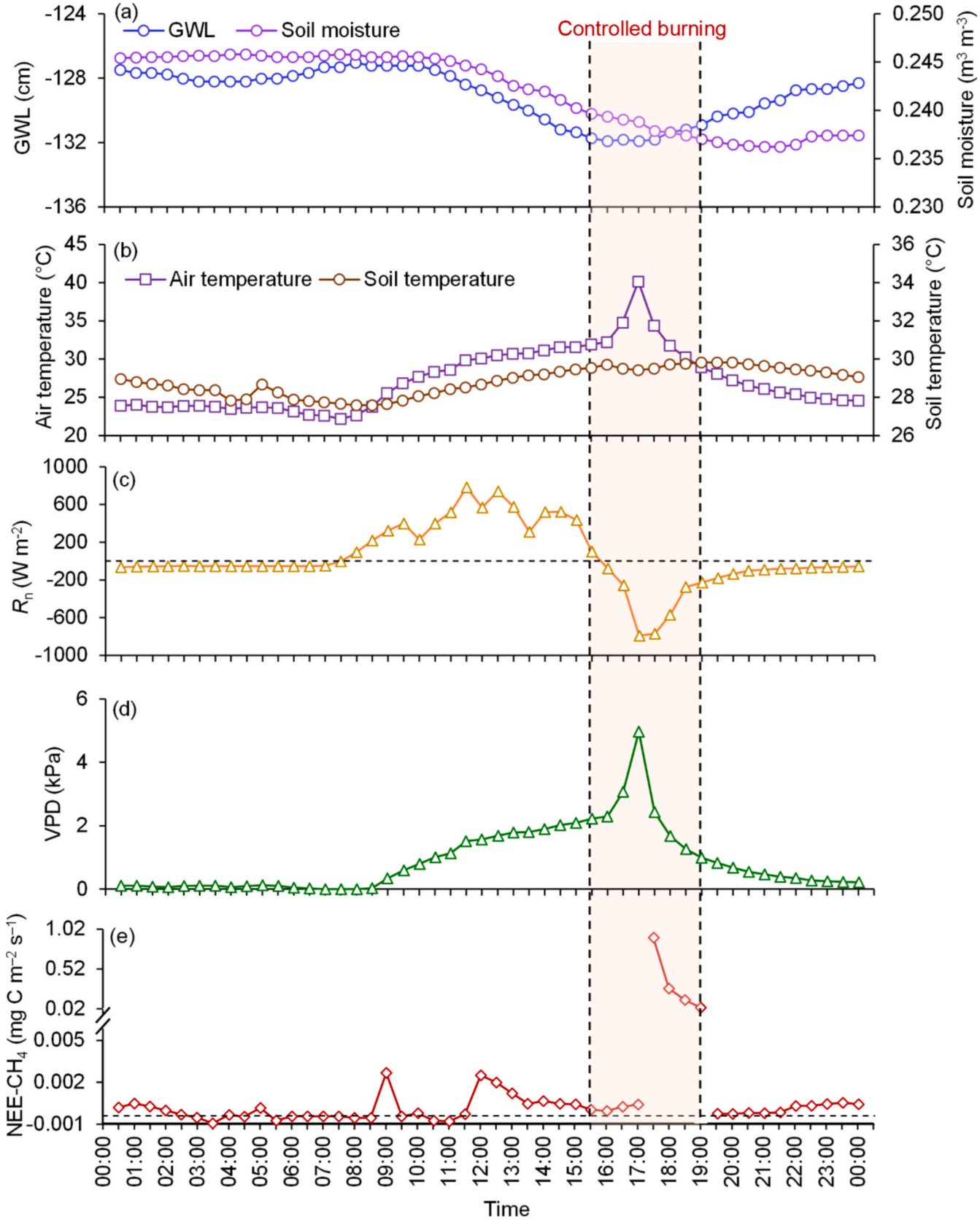

Fig. 5. Diurnal variations in (a) groundwater level (GWL) and soil moisture (30 cm depth), (b) air temperature and soil temperature (5 cm depth), (c) net radiation (R_n), (d) daytime vapor pressure deficit and (e) net ecosystem exchange of CH_4 (NEE-CH_4) on 17 February 2018. The horizontal dashed lines indicate zero lines.

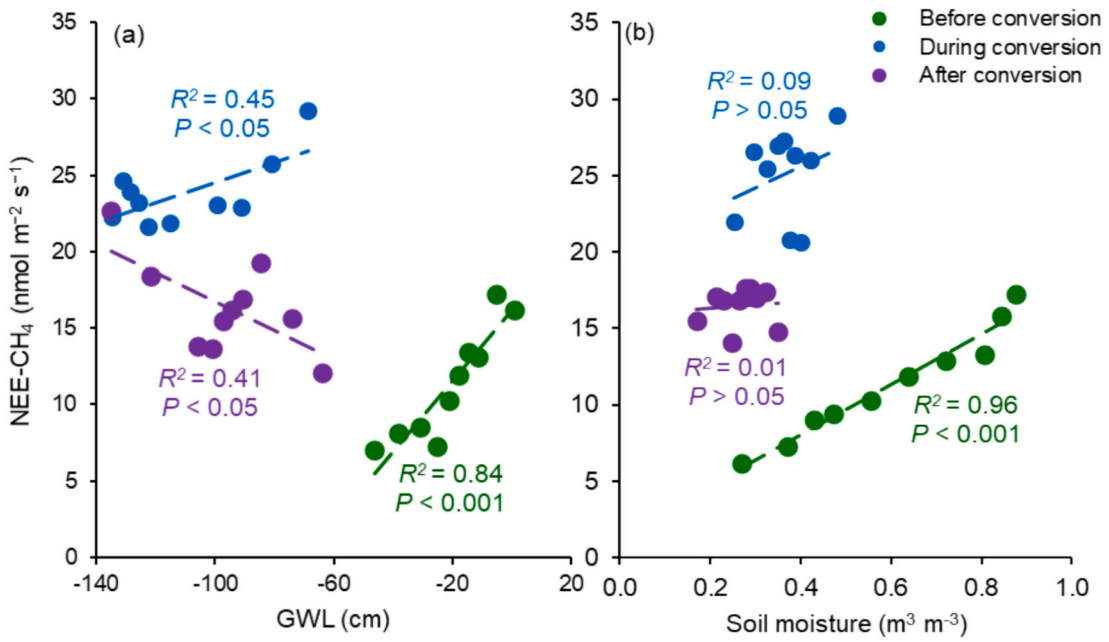

Fig. 6. Relationships of net ecosystem exchange of CH_4 (NEE-CH_4) with (a) groundwater level (GWL) and (b) soil moisture. Half hourly fluxes were rank-ordered and binned into 10 groups by each variable. The linear regression was fitted for the GWL and soil moisture.

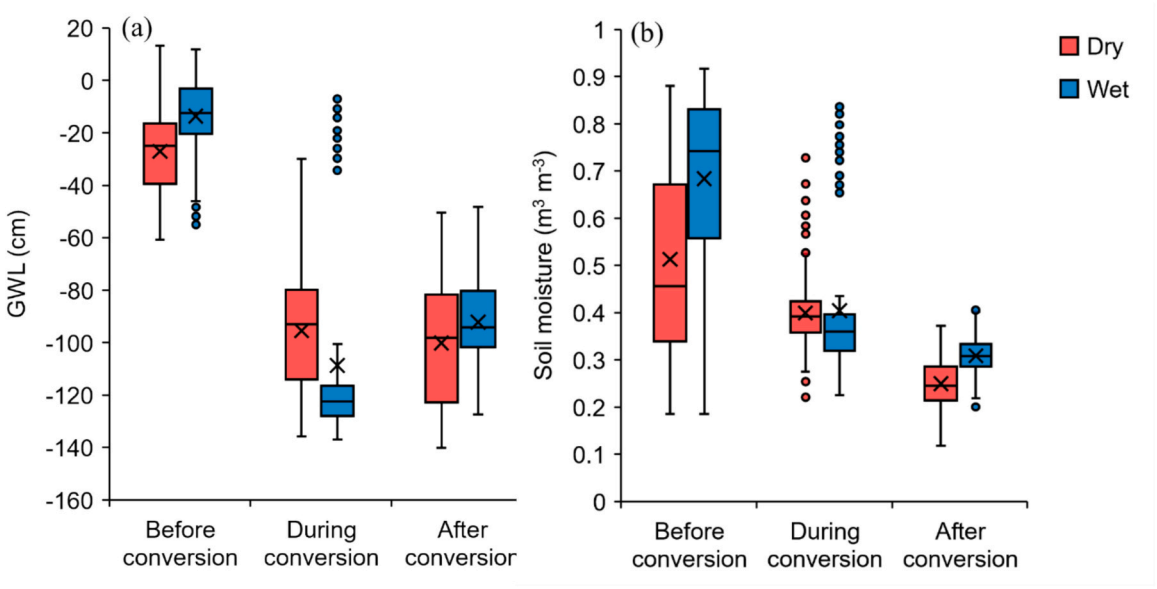

Fig. 7. Distribution of daily (a) GWL and (b) soil moisture (30 cm depth) during the dry (April – September) and wet (October – March) seasons before, during and after conversion. The boxes represent the interquartile ranges, whiskers represent the 1.5 times the interquartile range, black lines within the boxes represent the median values, "x" mark the mean values, while the blue and red dots represent the extreme values.

of forest cover along with drainage that dries the soil surface, leading to a more reflective soil surface that increases upward shortwave radiation and albedo (data not shown). Several studies have investigated the soil reflectance, showing increased reflectance with soil drying (Baumgardner et al., 1986; Twomey et al., 1986; Matthias et al., 2000; Lobell and Asner, 2002). In addition, the relatively open canopies of the young oil palm trees after conversion allowed more solar radiation to reach the soil, which in turn heated the soil and increased upward longwave radiation. The combined effect of increased upward shortwave and longwave radiations subsequently resulted in a reduction in R_n.

4.2. Environmental response to controlled burning

Controlled burning significantly influences the peatland environment, as shown in Fig. 5. During the controlled burning, the GWL was maintained at −131 to −132 cm below the ground and remained unaffected by the burning. However, the heat produced by the burning caused a temporary warming effect, increasing the air temperature by 8 °C. Numerous studies have documented that higher air temperatures can increase VPD (Williams et al., 2013; Eamus et al., 2013; Will et al., 2013; Huang et al., 2019; Yuan et al., 2019). Consequently, the spike in air temperature resulted in a doubling of the VPD to 4.97 kPa. The smoke emitted during burning can attenuate the R_n by absorbing and

reflecting incoming radiation, while the burning contributes to surface warming and an increase in upward longwave radiation (Stone et al., 2008; Li et al., 2017; Várnai et al., 2019). Specifically, we observed an increase in upward shortwave radiation by 314 W m^{-2}, primarily due to smoke reflection, and an increase in upward longwave radiation by 657 W m^{-2} because of surface warming. The elevated upward radiations caused a marked decrease in R_n, with values descending into the negative during the period of controlled burning. The significant amount of charcoal generated during the controlled burning darkened the peatland surface (Fig. S2), consequently reducing albedo (data not shown) and altering R_n (Ohkubo et al., 2021). Soil moisture and temperature in the unburned area did not change attributable to the burning. In the burning area, it is logically inferred that heat generated by burning could penetrate deeper into the soil, potentially increasing soil temperatures, causing moisture vaporization, and reducing soil moisture content (Massman et al., 2010). Furthermore, the increase in air temperature, coupled with a higher VPD, leads to greater evaporative demand, which could further reduce the soil moisture (Seneviratne et al., 2010).

4.3. Peatland conversion and CH_4 emissions

Compared to a recent study in Sumatra, Indonesia (Deshmukh et al., 2020), our mean NEE-CH_4 value during conversion (Table 2) was double that of an Acacia plantation. After the conversion, our mean NEE-CH_4 was 43 % higher than the rate in the Acacia plantation cited in the same study.

While previous studies comparing peat swamp forests with agricultural plantations suggested that draining tropical peatlands for agriculture often leads to reduced CH_4 emissions (Melling et al., 2005; Wong et al., 2020; Swails et al., 2021, 2023), our results indicate a rise in CH_4 emissions during and after the conversion with drainage. This discrepancy indicates that the direct comparisons between the CH_4 fluxes of peat swamp forests and agricultural plantations in the earlier studies do not fully capture the effect of land conversion, potentially leading to a significant underestimation of the conversion-related CH_4 emissions. Furthermore, it is important to note that making direct comparisons of greenhouse gas fluxes between undisturbed forests and mature oil palm plantation emissions is not sufficient, as this fails to account for the emissions associated with the land conversion process (Cooper et al., 2020).

In waterlogged peatlands, anaerobic conditions favour methanogenesis, resulting in CH_4 supersaturation within the porewater of deep, anaerobic peat layers (Lai, 2009). When this supersaturation exceeds hydrostatic pressure, CH_4 bubbles form and can become trapped within peat pores (Chanton and Whiting, 1995; Kellner et al., 2005). Numerous studies have documented elevated concentrations of CH_4 in the deep layers of peat soils (Saarnio et al., 1997; Melling et al., 2005; Beer and Blodau, 2007; Münchberger et al., 2019; Yuan et al., 2021), with the potential for release at a high rate upon exposure to the atmosphere (Inubushi et al., 1998). Before conversion, soil CH_4 concentrations at the study site (sampled from stainless steel pipes) ranged from 2.4 to 56.5 ppm between 0 and 40 cm depth, increasing to 610 ppm at 80 cm depth. The land conversion process involved extensive excavation to establish drainage channels, penetrating the peat soil to depths of 1.2–2.5 m (Melling et al., 2008), which exposed deep peat layers to the atmosphere. The three peaks in monthly NEE-CH_4 (Fig. 3f) coincided with excavation period of the main and collection drains from March to September 2017, which may have contributed to a high rate of CH_4 release from the exposed deep peat layers. While waterlogged conditions hinder CH_4 diffusion, drainage during the initial stages of conversion can temporarily enhance diffusion, leading to increased CH_4 emissions (Moore and Roulet, 1993; Romanowicz et al., 1995; Mojeremane et al., 2010). Indeed, when the GWL is lowered, the hydrostatic pressure within the peat is reduced, increasing CH_4 ebullition (Männistö et al., 2019). Furthermore, mechanical disturbances of soil can release entrapped CH_4, increasing emissions via ebullition (Fechner-Levy and Hemond, 1996; Neue et al., 1997; Aulakh et al., 2001; Martínez-Eixarch et al., 2018). Due to the high porosity of peat soil, compaction reduces its pore space, forcing trapped gas bubbles to the surface, where they are released into the atmosphere. These disturbances, particularly clear-cutting and soil compaction, are likely contributing to the increase in CH_4 emissions observed during conversion.

Increase in CH_4 emissions after drainage both during and after conversion, largely due to the release of CH_4 from drainage ditches. In temperate peatlands, small water bodies, particularly drainage ditches, can act as hotspots for CH_4 emissions, contributing significantly to the total emissions (Minkkinen and Laine, 2006; Hendriks et al., 2007; Schrier-Uijl et al., 2010; Hyvönen et al., 2013; Köhn et al., 2021). Existing studies in tropical peatlands using floating chambers to measure CH_4 fluxes indicate that drainage ditches exhibit highly variable but generally much higher emissions compared to the surrounding peat areas, highlighting the ditches as potential hotspots for CH_4 emissions (Jauhiainen and Silvennoinen, 2012; Kent, 2019; Manning et al., 2019). A recent study by Kasak et al. (2023) discovered that the average CH_4 emissions originating from the study site's ditches reached 10.8 ± 14.3 mg C m^{-2} h^{-1}, accounting both diffusive and ebullitive emission types. Notably, this emission rate from the ditches was more than twice the rate reported for the mature oil palm plantations on peat in Bintulu, Sarawak (Manning et al., 2019). Furthermore, the spatial extent of ditches within the peatland has been shown to affect the CH_4 emissions (Evans et al., 2016), and our study site was moderately drained following the classification by Dadap et al. (2021). An analysis of the eddy covariance footprint (Kljun et al., 2015) revealed that 80 % of the fluxes after conversion originated within a 750 m radius upwind of the measurement point, predominantly originating from the oil palm plantation (Fig. S3). The drainage ditches were found to occupy 5.9 % of this flux footprint area. Notably, in a temperate peatland, a mere 5 % coverage by ditches can account for as much as 84 % of the total CH_4 emissions (Teh et al., 2011).

High CH_4 emissions from drainage ditches may arise from microbial decomposition of dissolved organic carbon (DOC) in the pore water of sediments or peat, or via lateral transport of dissolved CH_4 from anoxic peat layers (Billett and Moore, 2008; Clark et al., 2023; Dean et al., 2018). Although this study did not measure DOC concentrations, it has been reported that lowering the GWL through drainage enhances soil aeration, thereby increasing oxygen in the soil and accelerating the decomposition of organic matter, which can lead to increased dissolved organic carbon concentrations (Strack et al., 2008, 2019; Zhao et al., 2020; Bowen et al., 2024). These higher DOC concentrations provide a larger supply of carbon substrate that stimulates microbial metabolism, resulting in increased CH_4 production (Luan and Wu, 2015; Leng et al., 2021). As for the lateral transport, a large CH_4 efflux can occur from a ditch if CH_4-saturated water seeps from the adjacent peat into the ditch and is degassed (Turetsky et al., 2014), whereby the lateral transport of CH_4 is more feasible in tropical peatlands due to their high soil permeability (Baird et al., 2017; Kent, 2019).

After conversion, there was a decline in NEE-CH_4 from 2018 to 2020, as shown in Figs. 3f and 4. This trend might result from various factors, including the persistent drop in GWL, which increased aerobic decomposition of organic matter, consumed carbon substrates that would typically promote CH_4 production under anoxic conditions (Kettunen et al., 1999; Waddington and Day, 2007; Urbanová et al., 2013; Urbanová and Bárta, 2020). The consumption reduced available substrates for methanogenesis and decreased the CH_4 production potential. This dynamic is illustrated in Fig. 6a, where increases in GWL did not correlate with increased NEE-CH_4 after the conversion, suggesting that the available substrates may have been depleted over time due to the sustained lowering of GWL. Prolonged drying from drainage may also reduce the population and diversity of methanogens owing to oxygen toxicity (Yrjälä et al., 2011; Urbanová et al., 2013). In addition, the application of fertilizers such as nitrate and sulphate-based fertilizers to soil could suppress CH_4 emissions, disrupting the microbial

methanogenic processes. Some studies indicate that adding nitrate to soil can extensively utilize hydrogen by nitrate-reducing bacteria, inhibiting CH_4 production and potentially causing methanogenic toxicity (Klüber and Conrad, 1998; Roy and Conrad, 1999; Wang et al., 2018; Meng et al., 2023), while high sulphate fertilization rates may decrease CH_4 emissions due to sulphate-reducers outcompeting methanogens for substrates (Hori et al., 1990; Minamikawa et al., 2005). Furthermore, at the onset of an oil palm plantation, residual unburned coarse woody debris may act as a source of CH_4; however, this diminishes over time as the increasing populations of methanotrophs in the wood oxidize the CH_4, leading to reduced emissions from the decomposing wood (Mäkipää et al., 2018; Mukhortova et al., 2021; Hirano et al., 2022). Compared with a mature oil palm plantation (Wong et al., 2020), the annual NEE-CH_4 (5.6 g C m^{-2} $year^{-1}$) from the young oil palm plantation after conversion in this study was more than double, suggesting that CH_4 emissions could potentially decrease to less than half as the plantation matures, influenced by the aforementioned factors.

4.4. Controlled burning and CH_4 emissions

While the duration of controlled burning is short, it can lead to elevated values of NEE-CH_4, ranging from 0.04 to 0.91 mg C m^{-2} s^{-1} during this period (Fig. 5e). This increase could be attributable to the incomplete combustion of stacked woody debris, a process known to produce pyrogenic CH_4 (Stavert et al., 2022). However, it's important to note that our CH_4 measurements during controlled burning could be influenced by interference from elevated volatile organic compound (VOC) emissions, potentially affecting the accuracy of these elevated values (Kohl et al., 2019). Although this study was unable to directly address VOC interference, future research incorporating VOC measurements alongside CH_4 analysis would be valuable for determining the extent of this interference.

Despite the potential for VOC interference to influence the accuracy of short-term CH_4 flux measurements during controlled burning, we aimed to evaluate the overall effect of controlled burning on annual NEE-CH_4 during conversion. To do this, we calculated the annual emissions for the period of March 2017 to February 2018 under two scenarios: one reflecting a baseline condition where elevated values were omitted and gaps filled using the MDS method and another accounting for emissions including elevated values from controlled burning. The estimated NEE-CH_4 was 9.1 g C m^{-2} $year^{-1}$ for the baseline scenario, while including the elevated values from controlled burning raised the emission to 11.6 g C m^{-2} $year^{-1}$, demonstrating that controlled burning could potentially increase annual NEE-CH_4 by 26 %. A study examining the effect of slash-and-burn practices on a tropical peatland oil palm plantation found that burned areas emitted higher CH_4 than unburned areas (Dhandapani and Evers, 2020). Conversely, our study observed no significant rise in NEE-CH_4 in the months after the controlled burning (Fig. 3f). Indeed, the significant amount of pyrogenic carbon, which is charcoal formed during the incomplete burning in controlled burning, might affect subsequent microbial digestion processes. As CH_4 production in peat soils is predominantly facilitated by microbial digestion, the presence of pyrogenic carbon can modify these microbial activities, stimulate alternative forms of microbial respiration in the soil that limit CH_4 production (Sun et al., 2021).

4.5. Global warming potential of peatland conversion

Our results demonstrating increased CH_4 emissions from peatland conversion to oil palm plantations suggest the need for a comprehensive assessment of how these emissions impact the overall GWP of this land conversion. To this end, we calculated the GWP for each period (Table 3) using GWP factors of 1 for CO_2 and 27 for CH_4 over a 100-year timescale (IPCC, 2021). However, due to data constraints, our GWP assessments did not account for N_2O emissions, despite tropical peatlands being a significant source (Melling et al., 2007; Ishikura et al., 2018a). This omission could potentially result in an underestimation of the overall GWP.

Table 3
The annual net ecosystem exchange of CO_2 (NEE-CO_2) and CH_4 (NEE-CH_4), along with the global warming potential (GWP), was calculated for the periods before, during and after conversion. The GWP was based on radiative forcing over a 100-years' time horizon: $CO_2 = 1$ and $CH_4 = 27$.

Annual NEE	Before conversion (Peat swamp forest)	During conversion (Land clearing)	After conversion (Young oil palm plantation)
NEE-CO_2 (g CO_2 m^{-2} $year^{-1}$)[a]	293	9468	11,487
NEE-CH_4 (g CO_2-eq m^{-2} $year^{-1}$)	156	328	229
GWP (g CO_2-eq m^{-2} $year^{-1}$)	449	9797	11,716

[a] See details in Kiew et al. (2025).

Measurement of NEE-CO_2 at the same study site by Kiew et al. (2025) revealed that the NEE-CO_2 before, during and after conversion were 293, 9468 and 11,487 g CO_2 m^{-2} $year^{-1}$, respectively, denoting significant increases in CO_2 emissions throughout the conversion. In tandem, the NEE-CH_4 converted to CO_2 equivalents, were 156, 328 and 229 g CO_2-eq m^{-2} $year^{-1}$ for the respective time periods. Due to the conversion, the GWP increased markedly, reaching 9797 g CO_2-eq m^{-2} $year^{-1}$ during conversion and 11,716 g CO_2-eq m^{-2} $year^{-1}$ after conversion, compared to the before conversion value of 449 g CO_2-eq m^{-2} $year^{-1}$. The NEE-CH_4 accounted for 36 % of the GWP before conversion. In contrast, during and after conversion, the GWP predominantly consisted of NEE-CO_2, contributed >95 %, while NEE-CH_4 accounted for only 3.35 % during conversion and 1.95 % after conversion. Thus, the contribution of NEE-CH_4 to the GWP of peatland conversion was relatively minor. In a mature oil palm plantation, for comparison, with an NEE-CO_2 of 3642 g CO_2 m^{-2} $year^{-1}$ and an NEE-CH_4 of 79 g CO_2-eq m^{-2} $year^{-1}$, the NEE-CH_4 accounted for 2.12 % of the GWP (Kiew et al., 2020; Wong et al., 2020). This was slightly higher than the NEE-CH_4 contribution observed in the young oil palm plantation after conversion in this study.

5. Conclusions

Since 1990, extensive tropical peatlands in Southeast Asia have undergone substantial conversion to oil palm plantations (Miettinen et al., 2016). To our knowledge, this study provides the first continuous, in situ measurements of both environmental conditions and CH_4 fluxes throughout the entire conversion period, providing valuable insights into the impacts of peat swamp forest conversion. Our results demonstrate that drainage, removal of forest cover through clear-cutting and controlled burning during peat swamp forest conversion to oil palm plantation significantly altered the environment, including reduced GWL and soil moisture, increased soil temperature and altered radiation dynamics. Contrary to expectations that drainage would lower CH_4 emissions, our findings show that the site remained a consistent net source, with even higher emissions observed during and after conversion. Given these findings, this study makes a significant contribution by quantifying NEE-CH_4 emissions throughout peat swamp forest conversion to oil palm plantations. This data will ultimately contribute to improving global CH_4 inventories and flux observations. However, to gain a more thorough understanding of how this land conversion impacts CH_4 dynamics, further research, particularly investigating the changes in soil's physical and chemical properties and their correlation to CH_4 emissions, is needed.

CRediT authorship contribution statement

Guan Xhuan Wong: Methodology, Formal analysis, Writing – original draft, Data curation. **Ryuichi Hirata:** Methodology, Writing – review & editing. **Takashi Hirano:** Methodology, Writing – review & editing. **Frankie Kiew:** Writing – review & editing. **Joseph Wenceslaus Waili:** Writing – review & editing. **Ülo Mander:** Funding acquisition, Writing – review & editing. **Kaido Soosaar:** Funding acquisition, Writing – review & editing. **Lulie Melling:** Funding acquisition, Writing – review & editing.

Declaration of competing interest

The authors declare that they have no known competing financial interests or personal relationships that could have appeared to influence the work reported in this paper.

Acknowledgements

This study was supported by both the Sarawak State Government and the Government of Malaysia. We extend our gratitude to the staff at the Sarawak Tropical Peat Research Institute for their valuable assistance with the fieldwork. Our thanks also go to the Malaysian Meteorological Department and the Department of Irrigation and Drainage, Sarawak, for their cooperation in providing meteorological data. This work was also supported by the Estonian Research Council (PRG2032), and the European Union Horizon programme under grant agreement No. 101079192 (MLTOM23003R) and the European Research Council (ERC) under grant agreement No. 101096403 (MLTOM23415R).

Appendix A. Supplementary data

Supplementary data to this article can be found online at https://doi.org/10.1016/j.scitotenv.2025.178466.

Data availability

The data that has been used is confidential.

References

Adhi, Y.A., Mubarak, H., Roland, R., Utama, P.P., Tambusai, N., Ismail, I., Tarigan, s.D., Anwar, S., Sahari, B., 2021. Effects of rainfall and groundwater level on soil subsidence, water content, and yield of oil palm. In IOP Conference Series: Earth and Environmental Science 771, 012029. https://doi.org/10.1088/1755-1315/771/1/012029.

Alberto, M.C.R., Wassmann, R., Buresh, R.J., Quilty, J.R., Correa Jr., T.Q., Sandro, J.M., Centeno, C.A.R., 2014. Measuring methane flux from irrigated rice fields by eddy covariance method using open-path gas analyzer. Field Crop Res. 160, 12–21. https://doi.org/10.1016/j.fcr.2014.02.008.

Anamulai, S., Sanusi, R., Zubaid, A., Lechner, A.M., Ashton-Butt, A., Azhar, B., 2019. Land use conversion from peat swamp forest to oil palm agriculture greatly modifies microclimate and soil conditions. PeerJ 7, e7656. https://doi.org/10.7717/peerj.7656.

Aubinet, M., Vesala, T., Papale, D. (Eds.), 2012. Eddy Covariance: A Practical Guide to Measurement and Data Analysis. Springer Science & Business Media.

Aulakh, M.S., Wassmann, R., Rennenberg, H., 2001. Methane Emissions from Rice Fields—Quantification, Mechanisms, Role of Management, and Mitigation Options. https://doi.org/10.1016/S0065-2113(01)70006-5.

Baird, A.J., 1997. Field estimation of macropore functioning and surface hydraulic conductivity in a fen peat. Hydrol. Process. 11 (3), 287–295. https://doi.org/10.1002/(SICI)1099-1085(19970315)11:3<287::AID-HYP443>3.0.CO;2-L.

Baird, A.J., Low, R., Young, D., Swindles, G.T., Lopez, O.R., Page, S., 2017. High permeability explains the vulnerability of the carbon store in drained tropical peatlands. Geophys. Res. Lett. 44 (3), 1333–1339. https://doi.org/10.1002/2016GL072245.

Bansal, S., Post van der Burg, M., Fern, R.R., Jones, J.W., Lo, R., McKenna, O.P., Tangen, B.A., Zhang, Z., Gleason, R.A., 2023. Large increases in methane emissions expected from North America's largest wetland complex. *Science*. Advances 9 (9), eade1112. https://doi.org/10.1126/sciadv.ade1112.

Basu, S., Lan, X., Dlugokencky, E., Michel, S., Schwietzke, S., Miller, J.B., Manca, G., 2022. Estimating emissions of methane consistent with atmospheric measurements of methane and δ 13 C of methane. Atmos. Chem. Phys. 22 (23), 15351–15377. https://doi.org/10.5194/acp-22-15351-2022.

Baumgardner, M.F., Silva, L.F., Biehl, L.L., Stoner, E.R., 1986. Reflectance properties of soils. Adv. Agron. 38, 1–44. https://doi.org/10.1016/S0065-2113(08)60672-0.

Beer, J., Blodau, C., 2007. Transport and thermodynamics constrain belowground carbon turnover in a northern peatland. Geochim. Cosmochim. Acta 71 (12), 2989–3002. https://doi.org/10.1016/j.gca.2007.03.010.

Billett, M.F., Moore, T.R., 2008. Supersaturation and evasion of CO_2 and CH_4 in surface waters at Mer Bleue peatland. Canada. Hydrol. Process. Int. J. 22 (12), 2044–2054. https://doi.org/10.1002/hyp.6805.

Bowen, J.C., Wahyudio, P.J., Anshari, G.Z., Aluwihare, L.I., Hoyt, A.M., 2024. Canal networks regulate aquatic losses of carbon from degraded tropical peatlands. Nat. Geosci. 17 (3), 213–218. https://doi.org/10.1038/s41561-024-01383-8.

Burba, G., Anderson, T., Komissarov, A., 2019. Accounting for spectroscopic effects in laser-based open-path eddy covariance flux measurements. Glob. Chang. Biol. 25 (6), 2189–2202. https://doi.org/10.1111/gcb.14614.

Cael, B.B., Goodwin, P.A., 2023. Global methane pledge versus carbon dioxide emission reduction. Environ. Res. Lett. 18 (10), 104015. https://doi.org/10.1088/1748-9326/acf8dd.

Cain, M., Jenkins, S., Allen, M.R., Lynch, J., Frame, D.J., Macey, A.H., Peters, G.P., 2022. Methane and the Paris agreement temperature goals. Phil. Trans. R. Soc. A 380 (2215), 20200456. https://doi.org/10.1098/rsta.2020.0456.

Carlson, K.M., Goodman, L.K., May-Tobin, C.C., 2015. Modeling relationships between water table depth and peat soil carbon loss in southeast Asian plantations. Environ. Res. Lett. 10 (7), 074006. https://doi.org/10.1088/1748-9326/10/7/074006.

Chanton, J.P., Whiting, G.J., 1995. Trace gas exchange in freshwater and coastal marine environments: Ebullition and transport by plants. In: Matson, P.A., Harriss, R.C. (Eds.), Biogenic Trace Gases: Measuring Emissions from Soil and Water. Blackwell, Oxford, pp. 98–125.

Chilukoti, N., Xue, Y., 2021. An assessment of potential climate impact during 1948–2010 using historical land use land cover change maps. Int. J. Climatol. 41 (1), 295–315. https://doi.org/10.1002/joc.6621.

Clark, L., Strachan, I.B., Strack, M., Roulet, N.T., Knorr, K.H., Teickner, H., 2023. Duration of extraction determines CO_2 and CH_4 emissions from an actively extracted peatland in eastern Quebec. Canada. Biogeosciences 20 (3), 737–751. https://doi.org/10.5194/bg-20-737-2023.

Collins, W.J., Webber, C.P., Cox, P.M., Huntingford, C., Lowe, J., Sitch, S., Powell, T., 2018. Increased importance of methane reduction for a 1.5 degree target. Environ. Res. Lett. 13 (5), 054003. https://doi.org/10.1088/1748-9326/aab89c.

Cooper, H.V., Evers, S., Aplin, P., Crout, N., Dahalan, M.P.B., Sjogersten, S., 2020. Greenhouse gas emissions resulting from conversion of peat swamp forest to oil palm plantation. Nat. Commun. 11 (1), 407. https://doi.org/10.1038/s41467-020-14298-w.

Dadap, N.C., Hoyt, A.M., Cobb, A.R., Oner, D., Kozinski, M., Fua, P.V., Rao, K., Harvey, C.F., Konings, A.G., 2021. Drainage canals in southeast Asian peatlands increase carbon emissions. *Agu*. Advances 2 (1). https://doi.org/10.1029/2020AV000321 e2020AV000321.

Dargie, G.C., Lewis, S.L., Lawson, I.T., Mitchard, E.T., Page, S.E., Bocko, Y.E., Ifo, S.A., 2017. Age, extent and carbon storage of the Central Congo Basin peatland complex. Nature 542 (7639), 86–90. https://doi.org/10.1038/nature21048.

Dean, J.F., Middelburg, J.J., Röckmann, T., Aerts, R., Blauw, L.G., Egger, M., Dolman, A. J., 2018. Methane feedbacks to the global climate system in a warmer world. Rev. Geophys. 56 (1), 207–250. https://doi.org/10.1002/2017RG000559.

Delwiche, K.B., Knox, S.H., Malhotra, A., Fluet-Chouinard, E., McNicol, G., Feron, S., Jackson, R.B., 2021. FLUXNET-CH_4: A global, multi-ecosystem dataset and analysis of methane seasonality from freshwater wetlands. Earth Syst. Sci. Data Discuss. 2021, 1–111. https://doi.org/10.5194/essd-13-3607-2021.

Deshmukh, C.S., Julius, D., Evans, C.D., Nardi A.P., Susanto, Page, S.E., Desai, A.R., 2020. Impact of forest plantation on methane emissions from tropical peatland. Glob. Chang. Biol. 26 (4), 2477–2495. https://doi.org/10.1111/gcb.15019.

Dhandapani, S., Evers, S., 2020. Oil palm 'slash-and-burn' practice increases post-fire greenhouse gas emissions and nutrient concentrations in burnt regions of an agricultural tropical peatland. Sci. Total Environ. 742, 140648. https://doi.org/10.1016/j.scitotenv.2020.140648.

Eamus, D., Boulain, N., Cleverly, J., Breshears, D.D., 2013. Global change-type drought-induced tree mortality: vapor pressure deficit is more important than temperature per se in causing decline in tree health. Ecol. Evol. 3 (8), 2711–2729. https://doi.org/10.1002/ece3.664.

Evans, C.D., Renou-Wilson, F., Strack, M., 2016. The role of waterborne carbon in the greenhouse gas balance of drained and re-wetted peatlands. Aquat. Sci. 78, 573–590. https://doi.org/10.1007/s00027-015-0447-y.

Fechner-Levy, E.J., Hemond, H.F., 1996. Trapped methane volume and potential effects on methane ebullition in a northern peatland. Limnol. Oceanogr. 41 (7), 1375–1383. https://doi.org/10.4319/lo.1996.41.7.1375.

Ferreira, T.R., Da Silva, B.B., De Moura, M.S., Verhoef, A., Nobrega, R.L., 2020. The use of remote sensing for reliable estimation of net radiation and its components: a case study for contrasting land covers in an agricultural hotspot of the Brazilian semiarid region. Agric. For. Meteorol. 291, 108052. https://doi.org/10.1016/j.agrformet.2020.108052.

Foken, T., Wichura, B., 1996. Tools for quality assessment of surface-based flux measurements. Agric. For. Meteorol. 78 (1–2), 83–105. https://doi.org/10.1016/0168-1923(95)02248-1.

Furukawa, Y., Inubushi, K., Ali, M., Itang, A.M., Tsuruta, H., 2005. Effect of changing groundwater levels caused by land-use changes on greenhouse gas fluxes from tropical peat lands. Nutr. Cycl. Agroecosyst. 71, 81–91. https://doi.org/10.1007/s10705-004-5286-5.

Gumbricht, T., Roman-Cuesta, R.M., Verchot, L., Herold, M., Wittmann, F., Householder, E., Murdiyarso, D., 2017. An expert system model for mapping tropical wetlands and peatlands reveals South America as the largest contributor. Glob. Chang. Biol. 23 (9), 3581–3599. https://doi.org/10.1111/gcb.13689.

Gusmayanti, E.V.I., Anshari, G.Z., Pramulya, M., Ruliyansyah, A., 2019. CO_2 fluxes from drained tropical peatland used for oil palm plantation in relation to peat characteristics and crop age after planting. Biodiv. J. Biol. Divers. 20 (6). https://doi.org/10.13057/biodiv/d200622.

Hadi, A., Inubushi, K., Furukawa, Y., Purnomo, E., Rasmadi, M., Tsuruta, H., 2005. Greenhouse gas emissions from tropical peatlands of Kalimantan, Indonesia. Nutr. Cycl. Agroecosyst. 71, 73–80. https://doi.org/10.1007/s10705-004-0380-2.

Hamada, Y., Darung, U., Limin, S.H., Hatano, R., 2013. Characteristics of fire-generated gas emission observed during a large peatland fire in 2009 at Kalimantan, Indonesia. Atmos. Environ. 74, 177–181. https://doi.org/10.1016/j.atmosenv.2013.03.058.

Hardwick, S.R., Toumi, R., Pfeifer, M., Turner, E.C., Nilus, R., Ewers, R.M., 2015. The relationship between leaf area index and microclimate in tropical forest and oil palm plantation: Forest disturbance drives changes in microclimate. Agric. For. Meteorol. 201, 187–195. https://doi.org/10.1016/j.agrformet.2014.11.010.

Hendriks, D.M.D., Van Huissteden, J., Dolman, A.J., Van der Molen, M.K., 2007. The full greenhouse gas balance of an abandoned peat meadow. Biogeosciences 4 (3), 411–424. https://doi.org/10.5194/bg-4-411-2007.

Hirano, T., Segah, H., Harada, T., Limin, S., June, T., Hirata, R., Osaki, M., 2007. Carbon dioxide balance of a tropical peat swamp forest in Kalimantan. Indonesia. Global Change Biol. 13 (2), 412–425. https://doi.org/10.1111/j.1365-2486.2006.01301.x.

Hirano, T., Kusin, K., Limin, S., Osaki, M., 2014. Carbon dioxide emissions through oxidative peat decomposition on a burnt tropical peatland. Glob. Chang. Biol. 20 (2), 555–565. https://doi.org/10.1111/gcb.12296.

Hirano, T., Wong, G.X., Waili, J.W., San Lo, K., Kiew, F., Aeries, E.B., Hirata, R., Ishikura, K., Hayashi, M., Murata, S., Shiraishi, T., Melling, L., 2022. Carbon loss from aboveground woody debris generated through land conversion from a secondary peat swamp forest to an oil palm plantation. J. Agric. Meteorol. 78 (4), 137–146. https://doi.org/10.2480/agrmet.D-22-00003.

Holden, J., 2009. Topographic controls upon soil macropore flow. Earth Surf. Process. Landf. 34 (3), 345–351. https://doi.org/10.1002/esp.1726.

Hori, K., Inubushi, K., Matsumoto, S., Wada, H., 1990. Competition of acetic acid between methane formation and sulfate reduction in paddy soil. Japan. J. Soil Sci. Plant Nutri. 61 (6), 572–578.

Huang, M., Piao, S., Ciais, P., Peñuelas, J., Wang, X., Keenan, T.F., Janssens, I.A., 2019. Air temperature optima of vegetation productivity across global biomes. Nature Ecol. Evol. 3 (5), 772–779. https://doi.org/10.1038/s41559-019-0838-x.

Hyvönen, N.P., Huttunen, J.T., Shurpali, N.J., Lind, S.E., Marushchak, M.E., Heitto, L., Martikainen, P.J., 2013. The role of drainage ditches in greenhouse gas emissions and surface leaching losses from a cutaway peatland cultivated with a perennial bioenergy crop. Boreal Environ. Res. 18 (2), 109.

Imran, Y., Melling, L., Wong, G.X., Hatano, R., Inoue, T., Aeries, E.B., Goh, K.J., Mah, D. Y.S., 2022. Long term dynamics of surface fluctuation in a peat swamp forest in Sarawak. Malaysia. Environ. Res. Commun. 4 (4), 041001. https://doi.org/10.1088/2515-7620/ac6295.

Inubushi, K., Hadi, A., Okazaki, M., Yonebayashi, K., 1998. Effect of converting wetland forest to sago palm plantations on methane gas flux and organic carbon dynamics in tropical peat soil. Hydrol. Process. 12 (13–14), 2073–2080. https://doi.org/10.1002/(SICI)1099-1085(19981030)12:13/14<2073::AID-HYP720>3.0.CO;2-K.

IPCC, 2021. Climate Change 2021: the Physical Science Basis. Contribution of working group I to the sixth assessment report of the intergovernmental panel on climate change, *2*(1), 2391 [eds. Masson-Delmotte, V., Zhai, P., Pirani, A., Connors, S. L., Péan, C., Berger, S., … & Zhou, B.].

Ishikura, K., Darung, U., Inoue, T., Hatano, R., 2018a. Variation in soil properties regulate greenhouse gas fluxes and global warming potential in three land use types on tropical peat. Atmosphere 9 (12), 465. https://doi.org/10.3390/atmos9120465.

Ishikura, K., Hirano, T., Okimoto, Y., Hirata, R., Kiew, F., Melling, L., Aeries, E.B., Lo, K. S., Musin, K.K., Waili, J.W., Wong, G.X., Ishii, Y., 2018b. Soil carbon dioxide emissions due to oxidative peat decomposition in an oil palm plantation on tropical peat. Agric. Ecosyst. Environ. 254, 202–212. https://doi.org/10.1016/j.agee.2017.11.025.

Iwata, H., Kosugi, Y., Keisuke, O., Mano, M., Sakabe, A., Miyata, A., Takahashi, K., 2014. Cross-validation of open-path and closed-path eddy-covariance techniques for observing methane fluxes. Bound.-Layer Meteorol. 151, 95–118. https://doi.org/10.1007/s10546-013-9890-2.

Jackson, R.B., Saunois, M., Bousquet, P., Canadell, J.G., Poulter, B., Stavert, A.R., Bergamaschi, P., Niwa, Y., Segers, A., Tsuruta, A., 2020. Increasing anthropogenic methane emissions arise equally from agricultural and fossil fuel sources. Environ. Res. Lett. 15 (7), 071002. https://doi.org/10.1088/1748-9326/ab9ed2.

Jauhiainen, J., Silvennoinen, H., 2012. Diffusion GHG fluxes at tropical peatland drainage canal water surfaces. Suo 63 (3–4), 93–105.

Jauhiainen, J., Takahashi, H., Heikkinen, J.E., Martikainen, P.J., Vasander, H., 2005. Carbon fluxes from a tropical peat swamp forest floor. Glob. Chang. Biol. 11 (10), 1788–1797. https://doi.org/10.1111/j.1365-2486.2005.001031.x.

Jauhiainen, J., Limin, S., Silvennoinen, H., Vasander, H., 2008. Carbon dioxide and methane fluxes in drained tropical peat before and after hydrological restoration. Ecology 89 (12), 3503–3514. https://doi.org/10.1890/07-2038.1.

Junedi, H., Armanto, M.E., Bernas, S.M., Imanudin, M.S., 2017. Changes to some physical properties due to conversion of secondary forest of peat into oil palm plantation. Sriwijaya J. Environ. 2 (3), 76–80. https://doi.org/10.22135/sje.2017.2.3.76-80.

Kang, M., Kim, J., Thakuri, B.M., Chun, J., Cho, C., 2019. Modification of the moving point test method for nighttime eddy CO_2 flux filtering on hilly and complex terrains. MethodsX 6, 1207–1217. https://doi.org/10.1016/j.mex.2019.05.012.

Kasak, K., Soosaar, K., Melling, L., Wong, G.X., Sangok, F., Ranniku, R., Villa, J., Sheel, B., Mander, Ü., 2023. Carbon emissions from drainage ditches in oil palm plantations on peat soil. AGU Fall Meeting Abstracts 1862, B51G–1862.

Kechavarzi, C., Dawson, Q., Leeds-Harrison, P.B., 2010. Physical properties of low-lying agricultural peat soils in England. Geoderma 154 (3–4), 196–202. https://doi.org/10.1016/j.geoderma.2009.08.018.

Kellner, E., Waddington, J.M., Price, J.S., 2005. Dynamics of biogenic gas bubbles in peat: potential effects on water storage and peat deformation. Water Resour. Res. 41 (8). https://doi.org/10.1029/2004WR003732.

Kent, M., 2019. *Greenhouse gas emissions from channels draining intact and degraded tropical peat swamp forest.* Open University (United Kingdom).

Kettunen, A., Kaitala, V., Lehtinen, A., Lohila, A., Alm, J., Silvola, J., Martikainen, P.J., 1999. Methane production and oxidation potentials in relation to water table fluctuations in two boreal mires. Soil Biol. Biochem. 31 (12), 1741–1749. https://doi.org/10.1016/S0038-0717(99)00093-0.

Kiew, F., Hirata, R., Hirano, T., Wong, G.X., Aeries, E.B., Musin, K.K., Waili, J.W., Lo, K. S., Shimizu, M., Melling, L., 2018. CO_2 balance of a secondary tropical peat swamp forest in Sarawak, Malaysia. Agric. For. Meteorol. 248, 494–501. https://doi.org/10.1016/j.agrformet.2017.10.022.

Kiew, F., Hirata, R., Hirano, T., Wong, G.X., Aeries, E.B., Musin, K.K., Wenceslaus, J., Lo, K.S., Shimizu, M., Melling, L., 2020. Carbon dioxide balance of an oil palm plantation established on tropical peat. Agric. For. Meteorol. 295, 108189. https://doi.org/10.1016/j.agrformet.2020.108189.

Kiew, F., Hirata, R., Hirano, T., Wong, G.X., Waili, J.W., Lo, K.S., Soosaar, K., Kasak, L., Mander, Ü., Melling, L., 2025. Carbon dioxide dynamics across three stages of tropical peatland conversion to oil palm plantations. [Manuscript in preparation].

Kljun, N., Calanca, P., Rotach, M.W., Schmid, H.P., 2015. A simple two-dimensional parameterisation for flux footprint prediction (FFP). Geosci. Model Dev. 8 (11), 3695–3713. https://doi.org/10.5194/gmd-8-3695-2015.

Klüber, H.D., Conrad, R., 1998. Effects of nitrate, nitrite, NO and N_2O on methanogenesis and other redox processes in anoxic rice field soil. FEMS Microbiol. Ecol. 25 (3), 301–318. https://doi.org/10.1111/j.1574-6941.1998.tb00482.x.

Knox, S.H., Jackson, R.B., Poulter, B., McNicol, G., Fluet-Chouinard, E., Zhang, Z., Zona, D., 2019. FLUXNET-CH_4 synthesis activity: objectives, observations, and future directions. Bull. Am. Meteorol. Soc. 100 (12), 2607–2632. https://doi.org/10.1175/BAMS-D-18-0268.1.

Kohl, L., Koskinen, M., Rissanen, K., Haikarainen, I., Polvinen, T., Hellén, H., Pihlatie, M., 2019. Interferences of volatile organic compounds (VOCs) on methane concentration measurements. Biogeosciences 16 (17), 3319–3332. https://doi.org/10.5194/bg-16-3319-2019.

Köhn, D., Welpelo, C., Günther, A., Jurasinski, G., 2021. Drainage ditches contribute considerably to the CH_4 budget of a drained and a rewetted temperate fen. Wetlands 41 (6), 1–15. https://doi.org/10.1007/s13157-021-01465-y.

Lai, D.Y.F., 2009. Methane dynamics in northern peatlands: a review. Pedosphere 19 (4), 409–421. https://doi.org/10.1016/S1002-0160(09)00003-4.

Lam, S.K., Goodrich, J.P., Liang, X., Zhang, Y., Pan, B., Schipper, L.A., Yiyi, S., Lee, N., Chen, D., 2022. Mitigating soil greenhouse-gas emissions from land-use change in tropical peatlands. Front. Ecol. Environ. 20 (6), 352–360. https://doi.org/10.1002/fee.2497.

Lan, X., Thoning, K.W., Dlugokencky, E.J., 2024. Trends in globally-averaged CH_4, N_2O, and SF_6 determined from NOAA global monitoring laboratory measurements. Version 2024-06. https://doi.org/10.15138/P8XG-AA10.

Laurance, W.F., Useche, D.C., 2009. Environmental synergisms and extinctions of tropical species. Conserv. Biol. 23 (6), 1427–1437. https://doi.org/10.1111/j.1523-1739.2009.01336.x.

Leng, P., Kamjunke, N., Li, F., Koschorreck, M., 2021. Temporal patterns of methane emissions from two streams with different riparian connectivity. *Journal of geophysical research.* Biogeosciences 126 (8). https://doi.org/10.1029/2020JG006104 e2020JG006104.

Li, F., Lawrence, D.M., Bond-Lamberty, B., 2017. Impact of fire on global land surface air temperature and energy budget for the 20th century due to changes within ecosystems. Environ. Res. Lett. 12 (4), 044014. https://doi.org/10.1088/1748-9326/aa6685.

Li-Cor Inc, 2010. Li-7700 Open Path CH_4 Analyzer Instruction Manual.

Lin, H., Chen, Y., Song, Q., Fu, P., Cleverly, J., Magliulo, V., Fan, Z., 2017. Quantifying deforestation and forest degradation with thermal response. Sci. Total Environ. 607, 1286–1292. https://doi.org/10.1016/j.scitotenv.2017.07.062.

Liu, Z., Liu, Y., Baig, M.H.A., 2019. Biophysical effect of conversion from croplands to grasslands in water-limited temperate regions of China. Sci. Total Environ. 648, 315–324. https://doi.org/10.1016/j.scitotenv.2018.08.128.

Lobell, D.B., Asner, G.P., 2002. Moisture effects on soil reflectance. Soil Sci. Soc. Am. J. 66 (3), 722–727. https://doi.org/10.2136/sssaj2002.7220.

Luan, J., Wu, J., 2015. Long-term agricultural drainage stimulates CH_4 emissions from ditches through increased substrate availability in a boreal peatland. Agric. Ecosyst. Environ. 214, 68–77. https://doi.org/10.1016/j.agee.2015.08.020.

Ma, S., Worden, J.R., Bloom, A.A., Zhang, Y., Poulter, B., Cusworth, D.H., Jacob, D.J., 2021. Satellite constraints on the latitudinal distribution and temperature sensitivity of wetland methane emissions. *Agu.* Advances 2 (3). https://doi.org/10.1029/2021AV000533 e2021AV000408.

Mäkipää, R., Leppänen, S.M., Munoz, S.S., Smolander, A., Tiirola, M., Tuomivirta, T., Fritze, H., 2018. Methanotrophs are core members of the diazotroph community in decaying Norway spruce logs. Soil Biol. Biochem. 120, 230–232. https://doi.org/10.1016/j.soilbio.2018.02.012.

Malley, C.S., Borgford-Parnell, N., Haeussling, S., Howard, I.C., Lefèvre, E.N., Kuylenstierna, J.C., 2023. A roadmap to achieve the global methane pledge. Environ. Res. Clim. 2 (1), 011003. https://doi.org/10.1088/2752-5295/acb4b4.

Manning, F.C., Kho, L.K., Hill, T.C., Cornulier, T., Teh, Y.A., 2019. Carbon emissions from oil palm plantations on peat soil. Front. Forests Glob. Change 2, 37. https://doi.org/10.3389/ffgc.2019.00037.

Männistö, E., Korrensalo, A., Alekseychik, P., Mammarella, I., Peltola, O., Vesala, T., Tuittila, E.S., 2019. Multi-year methane ebullition measurements from water and bare peat surfaces of a patterned boreal bog. Biogeosciences 16 (11), 2409–2421. https://doi.org/10.5194/bg-16-2409-2019.

Mano, M., Miyata, A., Yasuda, Y., Nagai, H., Yamada, T., Ono, K., Saito, M., Kobayashi, Y., 2007. Quality control for the open-path eddy covariance data. J. Agric. Meteorol. (Japan) 63 (3).

Martínez-Eixarch, M., Alcaraz, C., Viñas, M., Noguerol, J., Aranda, X., Prenafeta-Boldú, F.X., Ibáñez, C., 2018. Neglecting the fallow season can significantly underestimate annual methane emissions in Mediterranean rice fields. PLoS One 13 (5), e0198081. https://doi.org/10.1371/journal. pone.0198081.

Massman, W.J., 2000. A simple method for estimating frequency response corrections for eddy covariance systems. Agric. For. Meteorol. 104 (3), 185–198. https://doi.org/10.1016/S0168-1923(00)00164-7.

Massman, W.J., 2001. Reply to comment by Rannik on "A simple method for estimating frequency response corrections for eddy covariance systems". Agric. For. Meteorol. 107 (3), 247–251. https://doi.org/10.1016/S0168-1923(00)00237-9.

Massman, W.J., Frank, J.M., Mooney, S.J., 2010. Advancing investigation and physical modeling of first-order fire effects on soils. Fire Ecol. 6, 36–54. https://doi.org/10.4996/fireecology.0601036.

Matthias, A.D., Fimbres, A., Sano, E.E., Post, D.F., Accioly, L., Batchily, A.K., Ferreira, L. G., 2000. Surface roughness effects on soil albedo. Soil Sci. Soc. Am. J. 64 (3), 1035–1041. https://doi.org/10.2136/sssaj2000.6431035x.

McCarter, C.P.R., Rezanezhad, F., Quinton, W.L., Gharedaghloo, B., Lennartz, B., Price, J., Connon, R., Van Cappellen, P., 2020. Pore-scale controls on hydrological and geochemical processes in peat: implications on interacting processes. Earth Sci. Rev. 207, 103227. https://doi.org/10.1016/j.earscirev.2020.103227.

McCarthy, D.R., Brown, K.J., 2006. Soil respiration responses to topography, canopy cover, and prescribed burning in an oak-hickory forest in southeastern Ohio. For. Ecol. Manag. 237 (1–3), 94–102. https://doi.org/10.1016/j.foreco.2006.09.030.

McDermitt, D., Burba, G., Xu, L., Anderson, T., Komissarov, A., Riensche, B., Schedlbauer, J., Starr, G., Zona, D., Oechel, W., Oberbauer, S., 2011. A new low-power, open-path instrument for measuring methane flux by eddy covariance. Appl. Phys. B Lasers Opt. 102, 391–405. https://doi.org/10.1007/s00340-010-4307-0.

McNicol, G., Fluet-Chouinard, E., Ouyang, Z., Knox, S., Zhang, Z., Aalto, T., Jackson, R. B., 2023. Upscaling wetland methane emissions from the FLUXNET-CH4 Eddy covariance network (UpCH4 v1. 0): model development, network assessment, and budget comparison. *AGU*. Advances 4 (5). https://doi.org/10.1029/2023AV000956 e2023AV000956.

Meijide, A., Badu, C.S., Moyano, F., Tiralla, N., Gunawan, D., Knohl, A., 2018. Impact of forest conversion to oil palm and rubber plantations on microclimate and the role of the 2015 ENSO event. Agric. For. Meteorol. 252, 208–219. https://doi.org/10.1016/j.agrformet.2018.01.013.

Meinshausen, M., Lewis, J., McGlade, C., Gütschow, J., Nicholls, Z., Burdon, R., Cozzi, L., Hackmann, B., 2022. Realization of Paris agreement pledges may limit warming just below 2 C. Nature 604 (7905), 304–309. https://doi.org/10.5281/zenodo.5886866.

Melling, L., Hatano, R., Goh, K.J., 2005. Methane fluxes from three ecosystems in tropical peatland of Sarawak. Malaysia. Soil Biol. Biochem. 37 (8), 1445–1453. https://doi.org/10.1016/j.soilbio.2005.01.001.

Melling, L., Hatano, R., Goh, K.J., 2007. Nitrous oxide emissions from three ecosystems in tropical peatland of Sarawak. Malaysia. Soil Sci. Plant Nutri. 53 (6), 792–805. https://doi.org/10.1111/j.1747-0765.2007.00196.x.

Melling, L., Chua, K.H., Lim, K.H., 2008. Managing peat soils under oil palm. Agronomic Principles & Practices of Oil Palm Cultivation, ACT 2008, 461–488.

Melton, J.R., Wania, R., Hodson, E.L., Poulter, B., Ringeval, B., Spahni, R., Kaplan, J.O., 2013. Present state of global wetland extent and wetland methane modelling: conclusions from a model inter-comparison project (WETCHIMP). Biogeosciences 10 (2), 753–788. https://doi.org/10.5194/bg-10-753-2013.

Meng, X., Zhu, Z., Xue, J., Wang, C., Sun, X., 2023. Methane and nitrous oxide emissions from a temperate peatland under simulated enhanced nitrogen deposition. Sustainability 15 (2), 1010. https://doi.org/10.3390/su15021010.

Miettinen, J., Shi, C., Liew, S.C., 2016. Land cover distribution in the peatlands of peninsular Malaysia, Sumatra and Borneo in 2015 with changes since 1990. Glob. Ecol. Conserv. 6, 67–78. https://doi.org/10.1016/j.gecco.2016.02.004.

Minamikawa, K., Sakai, N., Hayashi, H., 2005. The effects of ammonium sulfate application on methane emission and soil carbon content of a paddy field in Japan. Agric. Ecosyst. Environ. 107 (4), 371–379. https://doi.org/10.1016/j.agee.2004.10.027.

Minkkinen, K., Laine, J., 2006. Vegetation heterogeneity and ditches create spatial variability in methane fluxes from peatlands drained for forestry. Plant Soil 285, 289–304. https://doi.org/10.1007/s11104-006-9016-4.

Mojeremane, W., Rees, R.M., Mencuccini, M., 2010. Effects of site preparation for afforestation on methane fluxes at Harwood Forest, NE England. Biogeochemistry 97, 89–107. https://doi.org/10.1007/s10533-009-9322-z.

Moore, T.R., Roulet, N.T., 1993. Methane flux: water table relations in northern wetlands. Geophys. Res. Lett. 20 (7), 587–590. https://doi.org/10.1029/93GL00208.

Mukhortova, L., Pashenova, N., Meteleva, M., Krivobokov, L., Guggenberger, G., 2021. Temperature sensitivity of CO_2 and CH_4 fluxes from coarse woody debris in northern boreal forests. Forests 12 (5), 624. https://doi.org/10.3390/f12050624.

Münchberger, W., Knorr, K.H., Blodau, C., Pancotto, V.A., Kleinebecker, T., 2019. Zero to moderate methane emissions in a densely rooted, pristine Patagonian bog–biogeochemical controls as revealed from isotopic evidence. Biogeosciences 16 (2), 541–559. https://doi.org/10.5194/bg-16-541-2019.

Neue, H.U., Wassmann, R., Kludze, H.K., Bujun, W., Lantin, R.S., 1997. Factors and processes controlling methane emissions from rice fields. Nutr. Cycl. Agroecosyst. 49, 111–117. https://doi.org/10.1023/A:1009714526204.

Nisbet, E.G., Jones, A.E., Pyle, J.A., Skiba, U., 2022. Rising methane: is there a methane emergency? Phil. Trans. R. Soc. A 380 (2215), 20210334. https://doi.org/10.1098/rsta.2021.0334.

Nisbet, E.G., Manning, M.R., Dlugokencky, E.J., Michel, S.E., Lan, X., Roeckmann, T., White, J.W.C., 2023. Atmospheric methane: comparison between methane's record in 2006–2022 and during glacial terminations. Global Biogeochem. Cycles 37 (8). https://doi.org/10.1029/2023GB007875 e2023GB007875.

Ohkubo, S., Hirano, T., Kusin, K., 2021. Influence of disturbances and environmental changes on albedo in tropical peat ecosystems. Agric. For. Meteorol. 301, 108348. https://doi.org/10.1016/j.agrformet.2021.108348.

Osaki, M., Tsuji, N. (Eds.), 2016. Tropical Peatland Ecosystems. Springer Japan. https://doi.org/10.1007/978-4-431-55681-7.

Page, S.E., Rieley, J.O., Banks, C.J., 2011. Global and regional importance of the tropical peatland carbon pool. Glob. Chang. Biol. 17 (2), 798–818. https://doi.org/10.1111/j.1365-2486.2010.02279.x.

Papale, D., Reichstein, M., Aubinet, M., Canfora, E., Bernhofer, C., Kutsch, W., Longdoz, B., Rambal, S., Valentini, R., Vesala, T., Yakir, D., 2006. Towards a standardized processing of net ecosystem exchange measured with eddy covariance technique: algorithms and uncertainty estimation. Biogeosciences 3 (4), 571–583. https://doi.org/10.5194/bg-3-571-2006.

Peng, S., Lin, X., Thompson, R.L., Xi, Y., Liu, G., Hauglustaine, D., Ciais, P., 2022. Wetland emission and atmospheric sink changes explain methane growth in 2020. Nature 612 (7940), 477–482. https://doi.org/10.1038/s41586-022-05447-w.

Potter, C.S., 1999. Terrestrial biomass and the effects of deforestation on the global carbon cycle: results from a model of primary production using satellite observations. BioScience 49 (10), 769–778. https://doi.org/10.2307/1313568.

Price, J., 1997. Soil moisture, water tension, and water table relationships in a managed cutover bog. J. Hydrol. 202 (1–4), 21–32. https://doi.org/10.1016/S0022-1694(97)00037-1.

R Core Team, 2021. R: A Language and Environment for Statistical Computing. R Foundation for Statistical Computing, Vienna, Austria. https://www.r-project.org/.

Ravishankara, A.R., Kulenstierna, J., Michalopoulou, E., Höglund-Isaksson, L., Zhang, Y., Seltzer, K., Ru, M., Castelino, R., Faluvegi, G., Naik, V., 2021. Global Methane Assessment: Benefits and Costs of Mitigating Methane Emissions. United Nations Environment Programme. https://www.unep.org/resources/report/global-methane-assessment-benefits-and-costs-mitigating-methane-emissions.

Reichstein, M., Falge, E., Baldocchi, D., Papale, D., Aubinet, M., Berbigier, P., Valentini, R., 2005. On the separation of net ecosystem exchange into assimilation and ecosystem respiration: review and improved algorithm. Glob. Chang. Biol. 11 (9), 1424–1439. https://doi.org/10.1111/j.1365-2486.2005.001002.x.

Rezanezhad, F., Price, J.S., Quinton, W.L., Lennartz, B., Milojevic, T., Van Cappellen, P., 2016. Structure of peat soils and implications for water storage, flow and solute transport: A review update for geochemists. Chem. Geol. 429, 75–84. https://doi.org/10.1016/j.chemgeo.2016.03.010.

Romanowicz, E.A., Siegel, D.I., Chanton, J.P., Glaser, P.H., 1995. Temporal variations in dissolved methane deep in the Lake Agassiz peatlands. Minnesota. Glob. Biogeochem. Cycles 9 (2), 197–212. https://doi.org/10.1029/95GB00634.

Rossita, A., Witono, A., Darusman, T., Lestari, D.P., Risdiyanto, I., 2018. Water table depth fluctuations during ENSO phenomenon on different tropical peat swamp forest land covers in Katingan, Indonesia. In IOP Conference Series: Earth and Environmental Science 129, 012001. https://doi.org/10.1088/1755-1315/129/1/012001.

Roy, R., Conrad, R., 1999. Effect of methanogenic precursors (acetate, hydrogen, propionate) on the suppression of methane production by nitrate in anoxic rice field soil. FEMS Microbiol. Ecol. 28 (1), 49–61. https://doi.org/10.1111/j.1574-6941.1999.tb00560.x.

Saarnio, S., Alm, J., Silvola, J., Lohila, A., Nykänen, H., Martikainen, P.J., 1997. Seasonal variation in CH 4 emissions and production and oxidation potentials at microsites on an oligotrophic pine fen. Oecologia 110, 414–422. https://doi.org/10.1007/s004420050176.

Sakabe, A., Itoh, M., Hirano, T., Kusin, K., 2018. Ecosystem-scale methane flux in tropical peat swamp forest in Indonesia. Glob. Chang. Biol. 24 (11), 5123–5136. https://doi.org/10.1111/gcb.14410.

Sangok, F.E., Sugiura, Y., Maie, N., Melling, L., Nakamura, T., Ikeya, K., Watanabe, A., 2020. Variations in the rate of accumulation and chemical structure of soil organic matter in a coastal peatland in Sarawak. Malaysia. Catena 184, 104244. https://doi.org/10.1016/j.catena.2019.104244.

Saunois, M., Stavert, A.R., Poulter, B., Bousquet, P., Canadell, J.G., Jackson, R.B., Zhuang, Q., 2020. The global methane budget 2000–2017. Earth Syst. Sci. Data Discuss. 2019, 1–136. https://doi.org/10.5194/essd-12-1561-2020.

Schrier-Uijl, A.P., Kroon, P.S., Leffelaar, P.A., Van Huissteden, J.C., Berendse, F., Veenendaal, E.M., 2010. Methane emissions in two drained peat agro-ecosystems with high and low agricultural intensity. Plant Soil 329, 509–520. https://doi.org/10.1007/s11104-009-0180-1.

Seneviratne, S.I., Corti, T., Davin, E.L., Hirschi, M., Jaeger, E.B., Lehner, I., Orlowsky, B., Teuling, A.J., 2010. Investigating soil moisture–climate interactions in a changing climate: A review. Earth Sci. Rev. 99 (3–4), 125–161. https://doi.org/10.1016/j.earscirev.2010.02.004.

Stavert, A.R., Saunois, M., Canadell, J.G., Poulter, B., Jackson, R.B., Regnier, P., Zhuang, Q., 2022. Regional trends and drivers of the global methane budget. Glob. Chang. Biol. 28 (1), 182–200. https://doi.org/10.1111/gcb.15901.

Stone, R.S., Anderson, G.P., Shettle, E.P., Andrews, E., Loukachine, K., Dutton, E.G., Schaaf, C., Roman III, M.O., 2008. Radiative impact of boreal smoke in the Arctic: observed and modeled. J. Geophys. Res. Atmos. 113 (D14). https://doi.org/10.1029/2007JD009657.

Strack, M., Waddington, J.M., Bourbonniere, R.A., Buckton, E.L., Shaw, K., Whittington, P., Price, J.S., 2008. Effect of water table drawdown on peatland dissolved organic carbon export and dynamics. Hydrol/ Process. Int. J. 22 (17), 3373–3385. https://doi.org/10.1002/hyp.6931.

Strack, M., Munir, T.M., Khadka, B., 2019. Shrub abundance contributes to shifts in dissolved organic carbon concentration and chemistry in a continental bog exposed to drainage and warming. Ecohydrology 12 (5), e2100. https://doi.org/10.1002/eco.2100.

SugaWara, M., 1979. Automatic calibration of the tank model/L'étalonnage automatique d'un modèle à cisterne. Hydrol. Sci. J. 24 (3), 375–388. https://doi.org/10.1080/02626667909491876.

Sun, T., Guzman, J.J., Seward, J.D., Enders, A., Yavitt, J.B., Lehmann, J., Angenent, L.T., 2021. Suppressing peatland methane production by electron snorkeling through pyrogenic carbon in controlled laboratory incubations. Nat. Commun. 12 (1), 4119. https://doi.org/10.1038/s41467-021-24350-y.

Swails, E., Hertanti, D., Hergoualc'h, K., Verchot, L., Lawrence, D., 2019. The response of soil respiration to climatic drivers in undrained forest and drained oil palm plantations in an Indonesian peatland. Biogeochemistry 142, 37–51. https://doi.org/10.1007/s10533-018-0519-x.

Swails, E., Hergoualc'h, K., Verchot, L., Novita, N., Lawrence, D., 2021. Spatio-temporal variability of peat CH_4 and N_2O fluxes and their contribution to peat GHG budgets in Indonesian forests and oil palm plantations. Front. Environ. Sci. 9, 617828. https://doi.org/10.3389/fenvs.2021.617828.

Swails, E., Drewer, J., Hartill, J., Comeau, L.P., Verchot, L.V., Hergoualc'h, K.A., 2023. Soil nitrous oxide and methane fluxes from a land-use change transition of primary forest to oil palm in an Indonesian peatland. Biogeochemistry 167, 363–381. https://doi.org/10.1007/s10533-023-01070-7.

Tang, A.C., Melling, L., Stoy, P.C., Musin, K.K., Aeries, E.B., Waili, J.W., Shimizu, M., Poulter, B., Hirata, R., 2020. A Bornean peat swamp forest is a net source of carbon dioxide to the atmosphere. Glob. Chang. Biol. 26 (12), 6931–6944. https://doi.org/10.1111/gcb.15332.

Teh, Y.A., Silver, W.L., Sonnentag, O., Detto, M., Kelly, M., Baldocchi, D.D., 2011. Large greenhouse gas emissions from a temperate peatland pasture. Ecosystems 14, 311–325. https://doi.org/10.1007/s10021-011-9411-4.

Tian, W., Wang, H., Xiang, X., Loni, P.C., Qiu, X., Wang, R., Huang, X., Tuovinen, O.H., 2023. Water table level controls methanogenic and methanotrophic communities and methane emissions in a Sphagnum-dominated peatland. Microbiol. Spect. 11 (5). https://doi.org/10.1128/spectrum.01992-23 e01992-23.

Turetsky, M.R., Kotowska, A., Bubier, J., Dise, N.B., Crill, P., Hornibrook, E.R., Wilmking, M., 2014. A synthesis of methane emissions from 71 northern, temperate, and subtropical wetlands. Glob. Chang. Biol. 20 (7), 2183–2197. https://doi.org/10.1111/gcb.12580.

Twomey, S.A., Bohren, C.F., Mergenthaler, J.L., 1986. Reflectance and albedo differences between wet and dry surfaces. Appl. Opt. 25 (3), 431–437. https://doi.org/10.1364/AO.25.000431.

Ueyama, M., Hirata, R., Mano, M., Hamotani, K., Harazono, Y., Hirano, T., Miyata, A., Takagi, K., Takahashi, Y., 2012. Influences of various calculation options on heat, water and carbon fluxes determined by open-and closed-path eddy covariance methods. Tellus Ser. B Chem. Phys. Meteorol. 64 (1), 19048. https://doi.org/10.3402/tellusb.v64i0.19048.

Urbanová, Z., Bárta, J., 2020. Recovery of methanogenic community and its activity in long-term drained peatlands after rewetting. Ecol. Eng. 150, 105852. https://doi.org/10.1016/j.ecoleng.2020.105852.

Urbanová, Z., Bárta, J., Picek, T., 2013. Methane emissions and methanogenic archaea on pristine, drained and restored mountain peatlands, Central Europe. Ecosystems 16, 664–677. https://doi.org/10.1007/s10021-013-9637-4.

Várnai, T., Gatebe, C., Gautam, R., Poudyal, R., Su, W., 2019. Developing an aircraft-based angular distribution model of solar reflection from wildfire smoke to aid satellite-based radiative flux estimation. Remote Sens. 11 (13), 1509. https://doi.org/10.3390/rs11131509.

Vickers, D., Mahrt, L., 1997. Quality control and flux sampling problems for tower and aircraft data. J. Atmos. Ocean. Technol. 14 (3), 512–526. https://doi.org/10.1175/1520-0426(1997)014<0512:QCAFSP>2.0.CO;2.

Voldoire, A., Royer, J.F., 2004. Tropical deforestation and climate variability. Clim. Dyn. 22, 857–874. https://doi.org/10.1007/s00382-004-0423-z.

Waddington, J.M., Day, S.M., 2007. Methane emissions from a peatland following restoration. *Journal of geophysical research*. Biogeosciences 112 (G3). https://doi.org/10.1029/2007JG000400.

Wallage, Z.E., Holden, J., 2011. Near-surface macropore flow and saturated hydraulic conductivity in drained and restored blanket peatlands. Soil Use Manag. 27 (2), 247–254. https://doi.org/10.1111/j.1475-2743.2011.00336.x.

Wang, J., Xu, T.T., Yin, L.C., Han, C., Deng, H., Jiang, Y.B., Zhong, W.H., 2018. Nitrate addition inhibited methanogenesis in paddy soils under long-term managements. Plant Soil Environ. 64 (8), 393–399. https://doi.org/10.17221/231/2018-PSE.

Webb, E.K., Pearman, G.I., Leuning, R., 1980. Correction of flux measurements for density effects due to heat and water vapour transfer. Q. J. R. Meteorol. Soc. 106 (447), 85–100. https://doi.org/10.1002/qj.49710644707.

Wilczak, J.M., Oncley, S.P., Stage, S.A., 2001. Sonic anemometer tilt correction algorithms. Bound.-Layer Meteorol. 99, 127–150. https://doi.org/10.1023/A:1018966204465.

Will, R.E., Wilson, S.M., Zou, C.B., Hennessey, T.C., 2013. Increased vapor pressure deficit due to higher temperature leads to greater transpiration and faster mortality during drought for tree seedlings common to the forest–grassland ecotone. New Phytol. 200 (2), 366–374. https://doi.org/10.1111/nph.12321.

Williams, A.P., Allen, C.D., Macalady, A.K., Griffin, D., Woodhouse, C.A., Meko, D.M., McDowell, N.G., 2013. Temperature as a potent driver of regional forest drought stress and tree mortality. Nat. Clim. Chang. 3 (3), 292–297. https://doi.org/10.1038/nclimate1693.

Wong, G.X., Hirata, R., Hirano, T., Kiew, F., Aeries, E.B., Musin, K.K., Waili, J.W., Lo, K. S., Melling, L., 2018. Micrometeorological measurement of methane flux above a tropical peat swamp forest. Agric. For. Meteorol. 256, 353–361. https://doi.org/10.1016/j.agrformet.2018.03.02.

Wong, G.X., Hirata, R., Hirano, T., Kiew, F., Aeries, E.B., Musin, K.K., Waili, J.W., Lo, K. S., Melling, L., 2020. How do land use practices affect methane emissions from tropical peat ecosystems? Agric. For. Meteorol. 282, 107869. https://doi.org/10.1016/j.agrformet.2019.107869.

Xu, J., Morris, P.J., Liu, J., Holden, J., 2018. PEATMAP: refining estimates of global peatland distribution based on a meta-analysis. Catena 160, 134–140. https://doi.org/10.1016/j.catena.2017.09.010.

Yrjälä, K.I.M., Tuomivirta, T., Juottonen, H., Putkinen, A., Lappi, K., Tuittila, E.S., Fritze, H., 2011. CH_4 production and oxidation processes in a boreal fen ecosystem after long-term water table drawdown. Glob. Chang. Biol. 17 (3), 1311–1320. https://doi.org/10.1111/j.1365-2486.2010.02290.x.

Yuan, F., Wang, Y., Ricciuto, D.M., Shi, X., Yuan, F., Hanson, P.J., Bridgham, S., Keller, J., Thornton, P.E., Xu, X., 2021. An integrative model for soil biogeochemistry and methane processes. II: warming and elevated CO_2 effects on peatland CH_4 emissions. *Journal of geophysical research*. Biogeosciences 126 (8). https://doi.org/10.1029/2020JG005963 e2020JG005963.

Yuan, W., Zheng, Y., Piao, S., Ciais, P., Lombardozzi, D., Wang, Y., Yang, S., 2019. Increased atmospheric vapor pressure deficit reduces global vegetation growth. *Science*. Advances 5 (8), eaax1396. https://doi.org/10.1126/sciadv.aax1396.

Zhang, Y., Wang, X., Yan, S., Zhu, J., Liu, D., Liao, Z., Li, C., Liu, Q., 2022. Influences of Phragmites australis density and groundwater level on soil water in semiarid wetland, North China: which is more influential? Ecohydrol. Hydrobiol. 22 (1), 85–95. https://doi.org/10.1016/j.ecohyd.2021.07.001.

Zhang, Z., Poulter, B., Feldman, A.F., Ying, Q., Ciais, P., Peng, S., Li, X., 2023. Recent intensification of wetland methane feedback. Nat. Clim. Chang. 13 (5), 430–433. https://doi.org/10.1038/s41558-023-01629-0.

Zhao, M., Han, G., Li, J., Song, W., Qu, W., Eller, F., Wang, J., Jiang, C., 2020. Responses of soil CO_2 and CH_4 emissions to changing water table level in a coastal wetland. J. Clean. Prod. 269, 122316. https://doi.org/10.1016/j.jclepro.2020.122316.

Zhao, S., Zhao, X., Li, Y., Chen, X., Li, C., Fang, H., Li, W., Guo, W., 2023. Impact of deeper groundwater depth on vegetation and soil in semi-arid region of eastern China. Front. Plant Sci. 14, 1186406. https://doi.org/10.3389/fpls.2023.1186406.

Zhu, S., McCalmont, J., Cardenas, L.M., Cunliffe, A.M., Olde, L., Signori-Müller, C., Litvak, M.E., Hill, T., 2023. Gap-filling carbon dioxide, water, energy, and methane fluxes in challenging ecosystems: comparing between methods, drivers, and gap-lengths. Agric. For. Meteorol. 332, 109365. https://doi.org/10.1016/j.agrformet.2023.109365.